College of Engineering
Electrical Engineering Department

EE497

Unleashing the PV Power Capabilities of the KSU Solar House

Students Team

Nzar Alhaidari **Student ID: 435108235**

Abdulaziz Alsanad **Student ID: 433104457**

Supervisors

Name	Signature
Prof. Mohamed Abuelela	**……**
Dr. Mohamed Abbas	**……**

Submitted in Partial Fulfillment of the Requirement

for the B.Sc. Degree,

Jumada'I 1442

December 2020

PROJECT ABSTRACT

The KSU solar house is a model house designed to be fully powered by a photovoltaic (PV) system. The house was constructed to participate in the 2018 edition of the Solar Decathlon Middle East (SDME) competition, which was held in Dubai in December 2018. The PV system of the house is grid-tied, and consists of PV modules rated for 18kWp. However, due to the regulations imposed by the competition, the output of the system is limited to only 8kW. Thus, while the installed inverters have a larger maximum capacity, they are programmed to limit their output to 8kW in order to satisfy the competition conditions.

The objective of this project is to utilize the installed capability of the PV system in a cost-efficient manner. This should be done without compromising the original goals of the solar house and should build upon the engineering work done on the original construction. Tools and materials should be reused from the initial construction effort where possible. A new design should be created based upon industry guidelines and simulation data. Testing and verification of the current system should be done before any modification. The new system should be tested and the data collected compared to the pre-modification system. The new system should be capable of remote monitoring. The performance of the new system should be judged based upon the metrics of power generation, energy yield, cost, and ease of maintenance.

During the design phase, the original Solar House project specifications were used as a base, alongside research of PV systems. A modified design was devised. This design would improve the performance of the PV system without undue cost and effort to install and maintain. The design would reuse much of the currently installed system and integrate seamlessly. Upon further inspection of the current system, and constructing additional models for simulation, it was found that the system was bottlenecked at the PV array, rather than at the solar inverters as the proposed design initially assumed. Thus, based upon this revelation, a different solution was chosen that would improve the performance of the PV system at a lower material cost.

After the design phase, the current system was tested and compared to the data collected from the SDME competition results. It was further compared to simulation data. Major discrepancies were found while testing the current system. After detailed inspection of the connections and wiring of the PV system, it was found that the PV system had been incorrectly installed and configured after being returned from the competition venue in Dubai. These issues were with the wiring and configuration of the system were rectified, and further data collected. It was also found that the solar modules had not been properly maintained, and were suffering from a large amount of dirt buildup on the surfaces. The modules were cleaned and a large increase in the generation was noted.

Data collection and aggregation was set up via an internet-connected portal that could be used to monitor and verify the PV system data. The firmware of all the installed hardware in the technical room, which had not been updated since the competition date, was updated. The software of the installed hardware was reconfigured to maximize power generation.

Finally, the limits imposed on the solar inverters during the competition were removed, and the performance of the system at its unleashed state measured. It was found that the power generation aligned closely with the expected data given the solar irradiance and simulation models. An online dashboard was built and deployed to collect and view the system data, which is automatically updated daily from the solar house.

ACKNOWLEDGEMENT

We would like to thank our parents for their continued support in our education.

We would also like to thank our supervisors, Dr. Mohamed Abbas and Prof. Mohamed Abuelela, for being an excellent source of knowledge and guidance during this project. We found their expertise and insight invaluable during the course of this project.

Lastly, we would like to acknowledge the support of the University for Projects such as the original Solar House, which gives students an opportunity to participate in real-world engineering projects during our studies.

TABLE OF CONTENTS

LIST OF FIGURES

LIST OF TABLES

1 INTRODUCTION

1.1 Problem Formulation

1.1.1 Problem Statement:

The PV system of the solar house is limited at the solar inverters to 8 kW, thus the system cannot access the full capacity of the installed PV array, which is 18 kWp. The system needs to be reconfigured to fully utilize the installed PV array. The wiring of the PV array and solar inverters will need to be adjusted, as will the settings of the inverters and other attached devices.

1.1.2 Problem Formulation:

The PV output of the solar house is currently limited to 8 kW whilst the installed PV array is rated for 18 kWp. The excess power generation capabilities of the PV array is currently wasted. By modifying the system, it should be possible to increase the AC output in order to utilize the entire capacity of the PV array.

1.2 Project Specifications

- The modified system should utilize the entire 18-kWp PV array.
- The modified system should be capable of remote monitoring and data collection.
- The modified system should build upon the original construction, reusing as much as possible.
- The modified system should increase the power generation and energy yield of the system.

2 BACKGROUND

2.1 Literature Review:

In modern times, sunlight has become an increasingly important source of electrical power. Fundamentally, solar cells depend upon the photovoltaic (PV) effect for their operation. This effect is caused by the unique electrical properties of semiconductor materials when exposed to light. A solar module is made by combining many such solar cells in one housing to create a single unit capable of generating electrical power, as shown in Figure 2.1. These solar modules generate electricity by converting sunlight directly into electricity [1].

Solar power is attractive for a variety of reasons. Firstly, it extracts energy from sunlight, and thus it is a renewable resource. There is no waste or pollution produced by this process, and so solar power is a clean source of energy. This is in stark contrast to fossil fuels, which produce large amounts of waste and pollution during both extraction and harvesting. Solar power is a clear answer to climate change, and the technology has been improving rapidly for decades [2].

Second, it is much cheaper in the long term than other sources of energy. Figure 2.2 shows how the price of solar modules is decreasing rapidly [3]; this decrease in cost is termed Swanson's law and it is analogous to Moore's law in integrated circuits. Aside from the initial upfront cost, a PV system requires minimal upkeep, making it an excellent option for residential power generation. This has great benefits for both the user and the power grid as a whole, alleviating peak demand and helping to accomplish peak load shaving. Solar power also has a long lifetime, with many modules offering guaranteed lifetimes of 25 years of constant service [4]. Selling excess power generated to the grid is also an option in situations where generation exceeds demand and a battery storage system is undesirable.

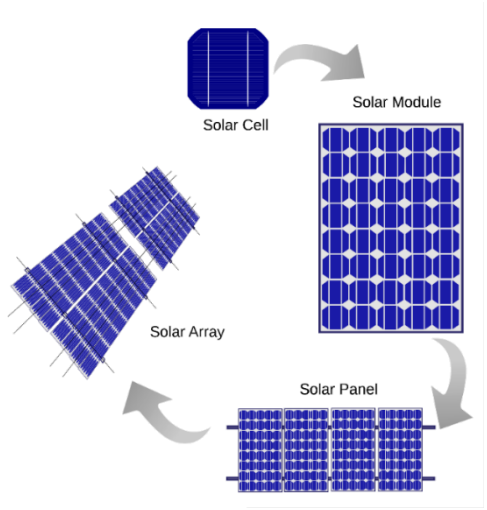

Figure 2.1 Solar cell to solar array

This allows for potential zero 'net-energy' consumption, where a home sells to the grid as much or more power than it purchases.

In terms of its electrical characteristics, solar modules generate direct current (DC) rather than the customary alternating current (AC) used in power grids. This has some benefits and some drawbacks. Because it is DC, it allows for easier storage in batteries whenever there is excess generation. However, because the majority of household devices are designed to run on AC, a device to convert DC to AC (called an inverter) is required to use the generated solar power in the home [5].

Because solar power is dependent on sunlight, it is only able to generate power when there is sunlight. This limits operation to certain times of the day, depending on the location and time of year. Thus, homes with PV systems have a need for an alternate source of power during the night. Some solar systems utilize battery storage to store excess energy produced during the day for nighttime use. Others use a grid-connected system where a traditional power grid is tapped when solar power production is not enough to satisfy demand. Other backup systems are also used, such as diesel-fueled generators, or other renewable energy sources (hydro, wind, geothermal, etc.). Systems that use both a battery storage solution and an emergency grid connection are also prevalent [5].

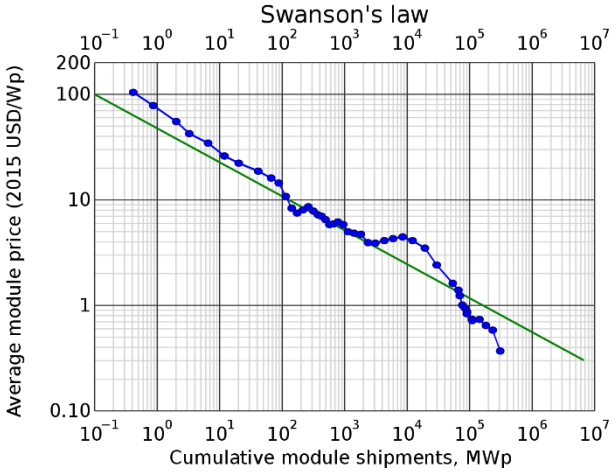

Figure 2.2 Swanson's Law for solar modules

2.1.1 PV System Design

Designing a PV system begins with identifying needs and constraints. The needs of a system can be deduced by answering the following questions:

I- How much power the system will be required to produce.
II- Whether the system will need a battery backup.
III- Whether the system will be connected to an external power grid.

Answering the first question requires knowledge of the loads that will be powered by the system. Table 1 shows the daily load power usage for a home. With this knowledge, a system designer can estimate the size of the PV system required to supply these loads for a certain amount of time. Because the system can only generate power during sunlight hours, the designer may choose to overprovision the solar array in order to charge a battery bank during the daylight hours [5]. This battery bank can then supply the loads when there is no sunlight.

An alternative to the battery backup is a grid connection. A grid connected PV system can sell excess power to the grid during sunlight hours, and purchase power from the grid during the nighttime. As long as the system sells to the grid more than it purchases, it will be net positive in terms of cost and energy generation. Both systems can be used in tandem as well, with the battery system being charged from the grid for example and being utilized as an emergency source if the grid is down.

The constraints are then related to the cost of the system and the site available for the system. In terms of costs, the type of module used and its efficiency plays a large role. A high quality mono-crystalline module with very good efficiency will be more expensive than a less efficient poly-crystalline module. The type of solar inverter and/or solar charge controller will also have an effect on the costs. A high efficiency inverter with a wide MPPT range will produce more energy in the long term but have a larger upfront cost. The costs of the supporting equipment such as mounting, cabling, and protection devices should be taken into account when comparing two systems.

Environmental concerns are a factor as well, a higher efficiency module means less total modules used for the same power production, reducing waste. Higher quality modules tend to have longer lifespans as well, meaning higher reliability in the long term.

The site available plays a very large role in the system design. Firstly, every location on earth has different sunlight hours. In addition, the sun will be at an angle relative to the latitude coordinate of the location, which will require the modules to be mounted at an angle for maximum generation [1]. The irradiation intensity of the sunlight will also be different at different locations. Second, the unobstructed area dictates how many solar modules can be placed. Third, the presence of shading from nearby structures can also affect generation [6]. Thus, it is very important to consider whether the location is suitable for a PV system before beginning the design process.

2.1.2 Design Example

Consider a home with daily load power usage[1] as in Table 1.

Table 1 Daily power consumption of common household appliances

Load	Power (W)	Daily Usage (hours)	Energy (kWh)
Refrigerator	140	8	1.12
Microwave	1200	0.5	0.6
Television	68	5	0.34
Lighting 1[2]	200	10	2
Lighting 2[3]	22	24	0.53
Electric Kettle	1500	.2	0.3
Air Conditioner	520	8	4.16
Ceiling Fan (x2)	100	6	0.6
Computer	120	6	0.72
Total	**3870**	**-**	**10.37**

The PV system for this home must supply 10.37 kWh of energy in one day to be self-sufficient. If we assume the sunlight hours suitable for generation in this location are six hours, then that means the PV system must generate the entirety of the annual daily energy usage in those six hours. This means that the PV system for our home must be able to generate:

$$\frac{10.37\ \text{kWh}}{6\ \text{hours}} = 1.73\text{kW}$$

Thus, the PV system needs to generate at least 1.73kW of power over those six hours of generation to satisfy the loads. If we assume system losses of 10%, and an inverter efficiency of 96%, we can calculate the power that must be supplied to the inverter to achieve this as:

$$\frac{1.73\text{kW}}{0.9} \times \frac{1}{0.96} = 2\text{kW}$$

Thus, the PV array size we need for this system is 2 kW. This will be enough to generate 10.37 kWh of energy per day, and satisfy the loads of the house.

However, this energy will be generated over six hours, while the house requires the energy over twenty-four hours. This means we require a battery system to store the energy generated for usage throughout the day.

To implement a battery system, we would need to account for the losses in charging and discharging a battery, which usually amount to 10% either way. Battery technology plays a role as well, with most chemical batteries requiring overprovisioning to maintain stability. Thus in our example, assuming a battery bank voltage of 48 V and depth of discharge of 80%, we would need batteries of capacity:

$$\frac{10.37\text{kWh}}{48\text{V}} \times \frac{1}{0.8^2} = 337.6\ \text{Ah}$$

Thus the battery bank would be made up of four 340 Ah 12V batteries connected in series, and would store enough energy to supply the home for an entire day.

[1] See Appendix for detailed load calculations.
[2] Lighting fixture with 20 LED bulbs.
[3] Lighting fixture with 4 LED bulbs.

2.1.3 Original Solar House Design

The hardware used in the original design consists of one Fronius Primo[1] solar inverter, one Victron Multiplus[1] inverter, and two Victron SmartSolar[1] charge controllers. Figure 2.4 shows the original arrangement, where inverter 1 refers to the Primo and inverter 2 refers to the Multiplus inverter.

The original design employed 60 290W Grie[1] solar modules, arranged in four strings as shown in Figure 7. The strings were connected to the solar inverters as shown in Figure 2.3. The two strings connected to inverter 1 directly via the two input ports present. The other two strings are each connected to one of the solar charge controllers, which have MPPT functionality. The output of the two charge controllers is then connected to both the two inputs of inverter 2 and the input of the batteries through a connection point.

The batteries are charged through the connection point, and are monitored via a smart battery monitor. This links them to the ESS of the Color Control, which controls their charge level.

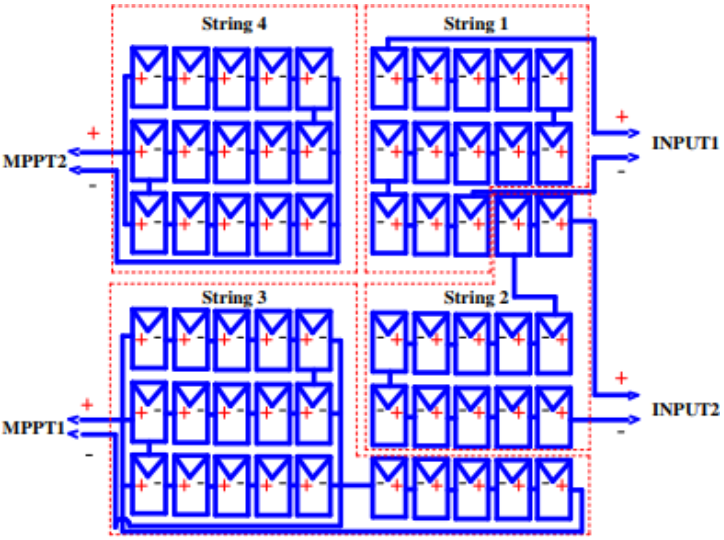

Figure 2.3 Original string configuration

The Victron Multiplus is connected through its AC bus to the local power grid. The system sells power to the grid through this connection when there is excess generation and the batteries are full, and purchases power when the PV generation and battery system cannot satisfy the loads.

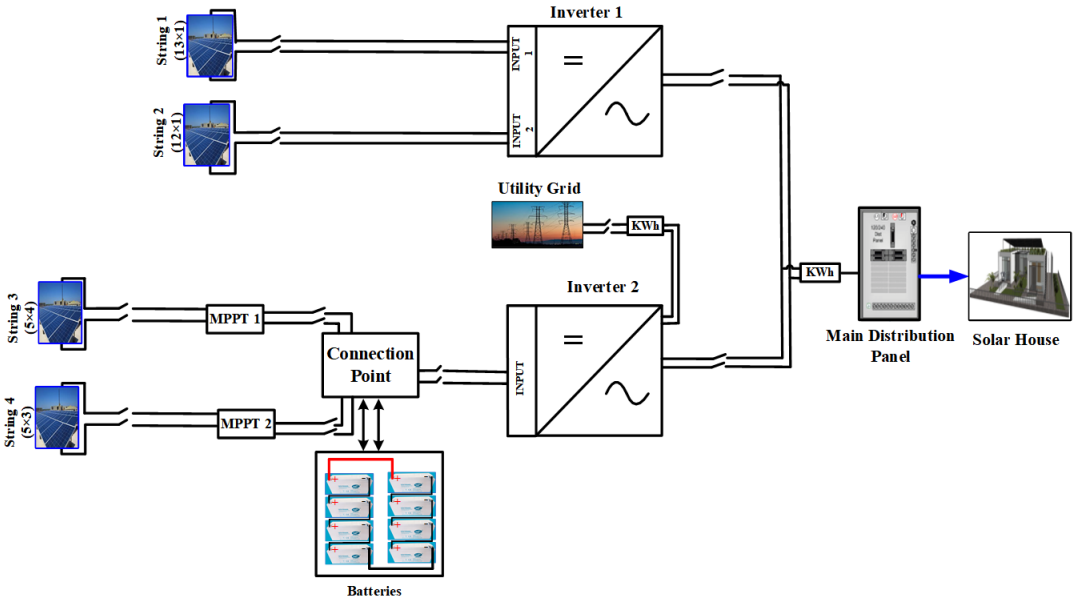

Figure 2.4 Original block diagram

[1] See Appendices for datasheets

2.2 Design Methods

2.2.1 Design tools and software used

For this project, we used a variety of software tools and programs, either to simulate systems, process data, or design systems. The tools used were:

- Microsoft Excel: A spreadsheet program. It was used to process raw data of simulation results and to produce graphs and charts.
- PVWatts: A web-based calculator made by NREL to estimate the energy production and cost of grid-connected PV systems. It was used to simulate solar irradiance and PV system collection and DC generation.
- HelioScope: A web-based PV design software. It was used for simulating the PV system collection, DC generation, and AC generation.
- Global Solar Atlas: The Global Solar Atlas is a collection of solar data and related solar energy assessment services, which provides access to solar resource and photovoltaic power potential data globally. It was used for analyzing the solar power potential at the solar house location.
- Autodesk AutoCAD: A CAD tool. It was used for drawing schematics, single line diagrams, and string configurations.
- Pandas: An open source data analysis and manipulation tool. It was used to process the raw data collected from the solar house.
- Streamlit: An open-source framework for creating data apps. It was used to build and deploy the online dashboard for the solar house.

2.3 Design Proposals

2.3.1 Modified design

2.3.1.1 Design Synthesis

When considering the problem, we had certain thoughts. The first thing we wanted was to retain as much of the original design as possible. This is for multiple reasons:

- It would allow us to reuse the proven and tested work of the original project.
- It would reduce the costs involved.
- It would lower the effort required for the upgrade

Thus, our first approach to the problem was in regards to the string arrangement. The original string arrangement (see Figure 7) overprovisioned both inverters. Inverter 1 was connected to 25 modules directly via two strings as in Table 2. Contrast the peak generation of 7.25kW with the inverter 1 AC output of 5 kW. By reducing the number of modules connected to this inverter, we can reuse them for our new upgrade. Reducing string 1 and string 2 to 10 modules each would still leave inverter 1 overprovisioned and free up 5 modules for our use in the upgrade. The total peak DC generation for inverter 1 post upgrade would thus be:

$$2\ \text{strings} \times (1 \times 10\ \text{modules/string}) \times 290\text{W/module} = 5800\text{W}$$

Table 2 Inverter 1 Original String Configuration

String	Number of modules in series	Number of strings in parallel	Total Modules	Peak DC generation at STC (W)
1	13	1	13	3770
2	12	1	12	3480
Total				7250

Similarly, inverter 2 was connected to 35 modules via four strings connected through the two solar charge controllers (see Figure 7). Table 3 shows the breakdown of per string generation and peak DC generation. Again, the total peak generation of 10.15kW is much larger than the AC output of inverter 2, which is limited to 3 kW.

Again, we see that by reducing the number of modules in string 3 and string 4 to 10 modules each, we can free up 15 modules for our use in the upgrade. The simplest way to do so is by reducing the number of strings in parallel, to maintain the voltage level required for the MPPT of the solar charge controllers.

Thus inverter 2 would be connected, via the two solar charge controllers, to 20 modules. Giving a total peak DC generation for inverter 2 post upgrade of:

$$2\ \text{strings} \times (2 \times 5\ \text{modules/string}) \times 290\text{W/module} = 5800\text{W}$$

This arrangement gives us 20 modules in total to use in our upgrade, and retain mostly the same wiring for the rest of the system.

Table 3 Inverter 2 Original String Configuration

String	Number of modules in series	Number of strings in parallel	Total Modules	Peak DC generation at STC (W)
3	5	4	20	5800
4	5	3	15	4350
Total				10150

2.3.1.2 Design Details

The new design will add a third inverter of the same type as inverter 1 to the system. This necessitates a change in the module string configuration. The new string configuration can be seen in Figure 8. The new inverter will be connected in parallel to the old system, at the same connection point between inverter 1 and 2 in Figure 6. The new single line diagram is shown in Figure 9.

In terms of the rest of the system, it will be mostly unchanged. The grid connection will stay as is, connected via inverter 2. The battery system likewise will be unchanged, connected to the outputs of the two solar charge controllers.

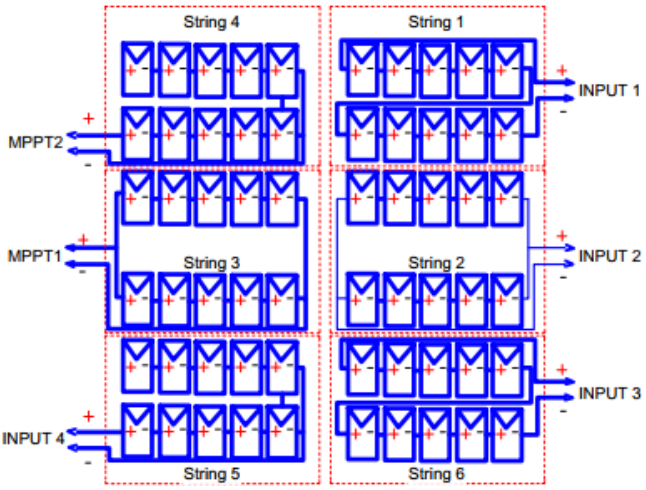

Figure 2.5 Modified string configuration

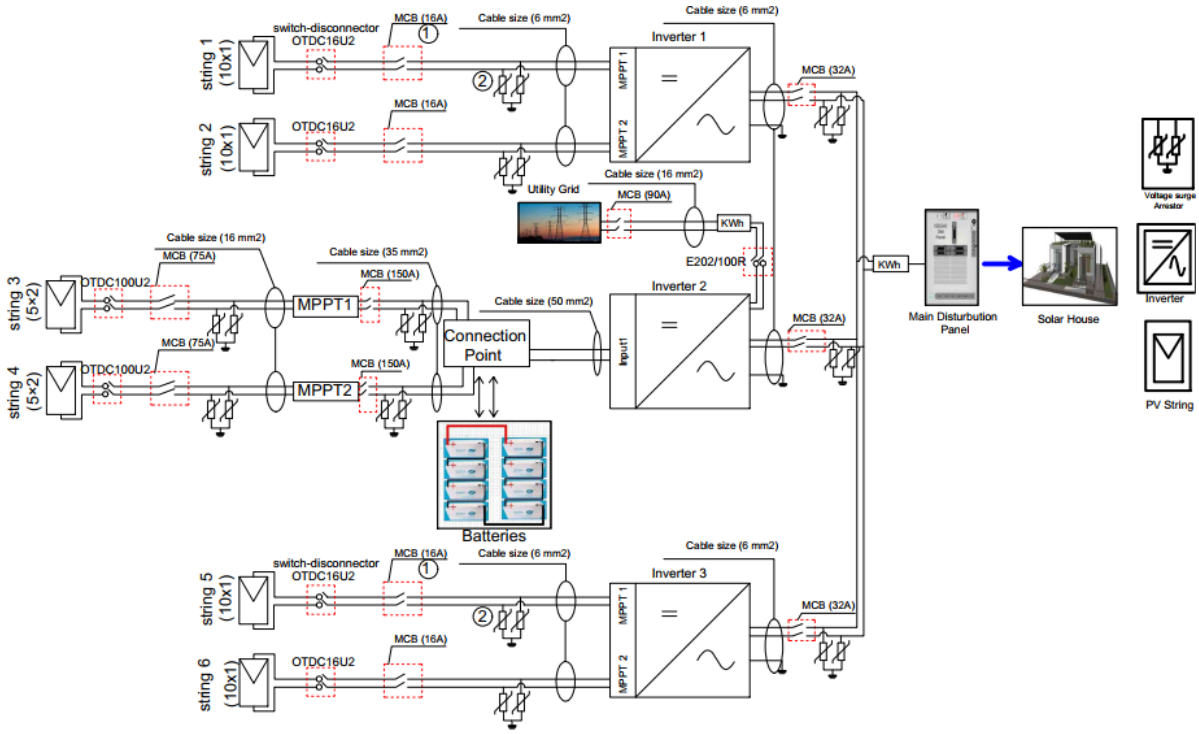

Figure 2.6 Modified block diagram

2.3.1.3 Design Safety Features

In terms of the protection circuitry, the new inverter will be connected via FG7R 0.6/1 kV PVC sheath cable according to the ampacity calculations in Table 4. Circuit breakers are used between elements. A disconnect switch is installed between the strings and the rest of the circuit. The new inverter is grounded via the same method as inverter 1.

Connection path	Thickness (mm^2)	Length. (M)	Current (A)	Cable Capacity (A)
PV string to Inverter1 inputs	6	8	9.384	14.3
Inverter1 output to MDB	6	5	21.74	31.25
Inverter2 output to MDB	6	5	21.74	31.25

Table 4 Cable capacity

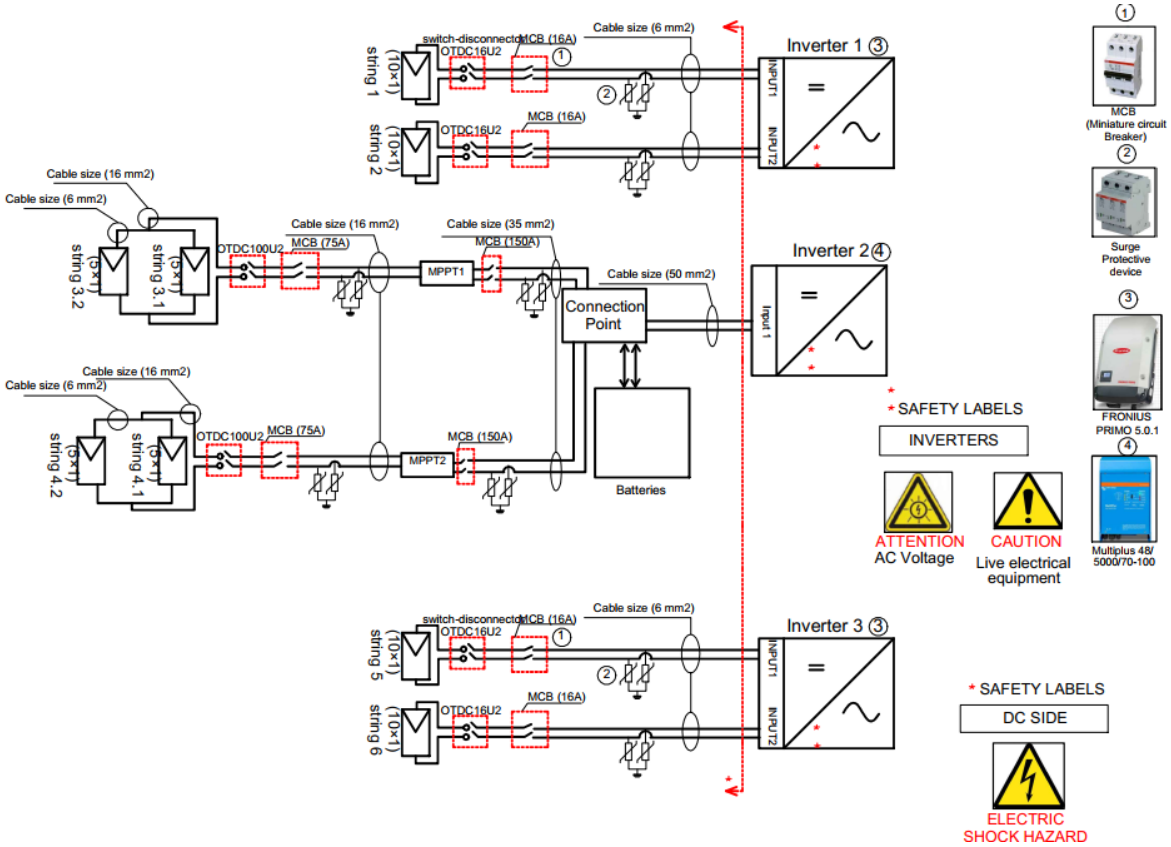

Figure 2.7 Modified DC circuit, showing protection circuity and string connections.

2.3.1.4 Design Simulation

2.3.1.4.1 Simulation setup & parameters

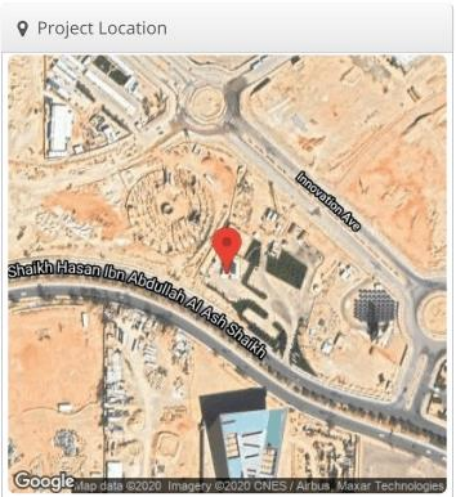

Figure 2.8 Setting location in

HelioScope:

Using HelioScope, the location was set to the KSU Solar House at its current location.

The array was set on the roof of the solar house, with 60 290w modules in total.

The strings were configured for three inverters, with the solar modules divided evenly between them.

Each inverter was thus connected to 20 x 290W = 5.8kW DC output at STC.

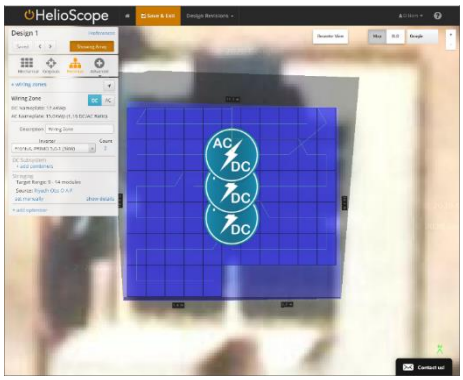

Figure 2.9 HelioScope electrical

PVWatts:

In PVWatts, the location was set to the Solar House roof, and the system info was entered, using the losses figures from HelioScope and the rated (average) inverter efficiency.

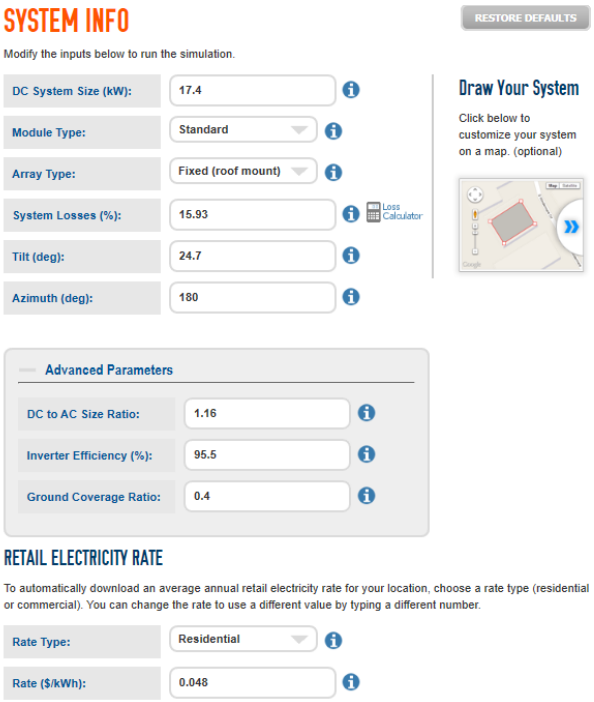

Figure 2.10 Entering system info in PVWatts

Figure 2.11 Setting location and array dimension in PVWatts

2.3.1.4.2 Simulation Results

The graph in Figure 18 shows the annual energy generation for the system. The peak is in the summer months when the solar irradiance is highest. As expected, the change in annual AC power generated is not as large as the change in AC output capacity. The largest increase in energy yield is during the peak months, when the solar irradiance is highest. On the other hand, when the solar irradiance is not enough to fully saturate the larger system, there is only a small difference in energy yield between the two.

Table 5 System output change due to modified design

	AC output capacity (kW)	**Simulated annual energy yield (Wh)**
Original System	8	26261.3
Modified System	15	29071.8
Change (%)	%87.5	%10.7

If we consider the value difference of the energy generated annually as in Figure 19, it amounts to 505.75 SR[1].

Annual Production

	Description	Output	% Delta
Irradiance (kWh/m²)	Annual Global Horizontal Irradiance	2,201.1	
	POA Irradiance	2,292.3	4.1%
	Shaded Irradiance	2,292.3	0.0%
	Irradiance after Reflection	2,220.7	-3.1%
	Irradiance after Soiling	2,176.3	-2.0%
	Total Collector Irradiance	**2,176.3**	**0.0%**
Energy (kWh)	Nameplate	37,804.5	
	Output at Irradiance Levels	37,726.5	-0.2%
	Output at Cell Temperature Derate	31,220.8	-17.2%
	Output After Mismatch	30,700.5	-1.7%
	Optimal DC Output	30,631.7	-0.2%
	Constrained DC Output	30,594.6	-0.1%
	Inverter Output	29,217.9	-4.5%
	Energy to Grid	**29,071.8**	**-0.5%**

Figure 2.12 HelioScope annual energy generation summary

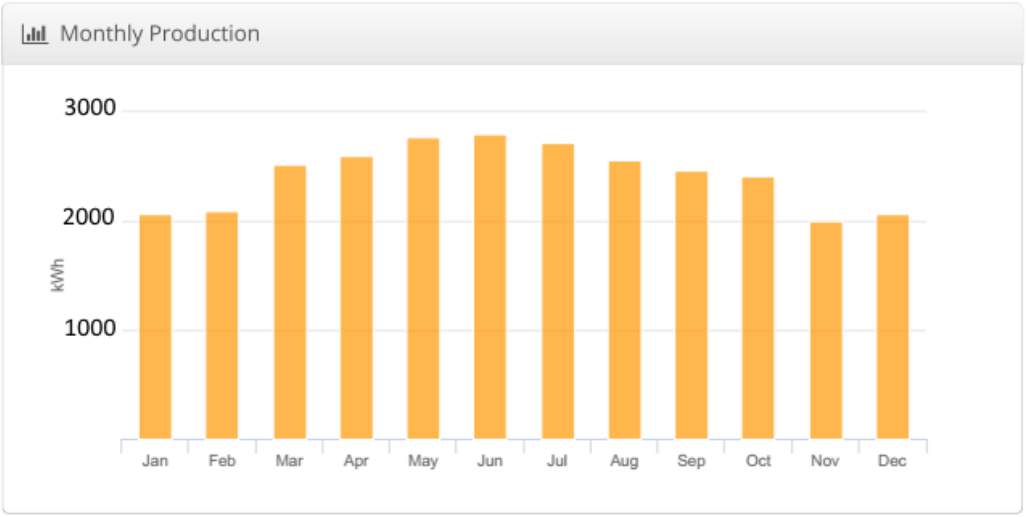

Figure 2.13 Monthly energy generation graph

[1] Value based upon the Saudi Electric Company consumption tariff of 0.18 SR/KWh. Annual energy yield difference between old and new system is: $29071.8\text{Wh} - 26261.298\text{Wh} = 2810.502\text{Wh}$ then multiplied by the tariff: $2810.502\text{Wh} \times 0.18\text{SR/kWh} = 505.75\text{SR}$

The main source of losses in the system is due to temperature. Temperatures in Riyadh regularly reach over 40° C in the summer, which has a hugely detrimental effect on solar module energy generation. As we can see in Figure 2.15, HelioScope calculates the average operating ambient temperature as 29.6 °C, which is considerably higher than the NOCT ambient temperature of 20 °C.

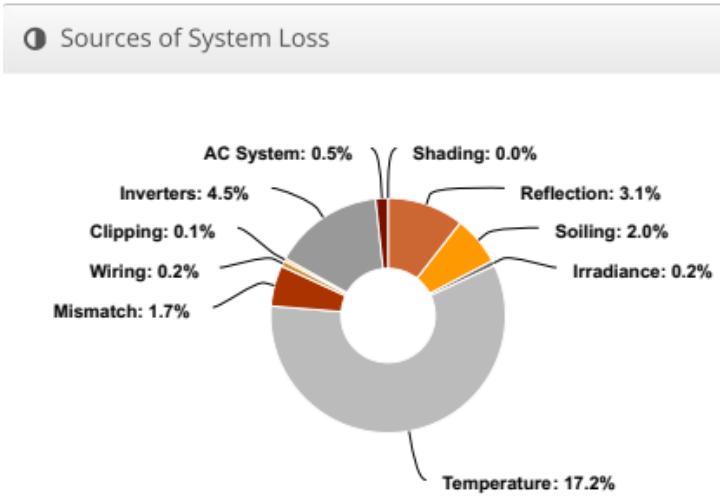

Figure 2.15 HelioScope simulation system losses

RESULTS **29,129 kWh/Year***

Month	Solar Radiation (kWh / m^2 / day)	AC Energy (kWh)	Value ($)
January	5.74	2,333	112
February	6.19	2,215	106
March	6.40	2,522	121
April	6.42	2,373	114
May	6.88	2,523	121
June	7.23	2,534	122
July	7.18	2,606	125
August	7.27	2,593	124
September	7.39	2,565	123
October	7.22	2,660	128
November	6.13	2,232	107
December	4.87	1,971	95
Annual	6.58	29,127	$ 1,398

Figure 2.14 PVWatts annual energy generation and value

2.3.1.5 Design Summary

We expect the change to result in an increase to the AC power generation of the system. Although the change in AC output capacity represents an 87.5%[1] increase, we do not expect the actual annual energy yield to change by this much. This is because the results will be dependent upon the solar irradiance expected, and for much of the year the larger system will not be saturated fully. That is to say, the inverter AC output of the current system is only a bottleneck in power generation when the solar irradiance is at its peak.

In total, the hardware required for the upgrade is summarized Table 5:

Solar Inverter		
Type	**Rating**	**Amount**
Fronius Primo 5.0.1	5kW	1
Cables		
Connection Path	**Length**	**Thickness**
PV string to inverter	8 m	6 mm^2
Inverter output to MDB	5 m	6 mm^2
Protection Equipment		
Type	**Rating**	**Amount**
Disconnect Switch	16 A	1
MCB	16 A	1
MCB	32 A	1
Voltage Surge Arrestor		1

Table 6 Hardware required

[1] $\frac{15-8}{8} = 0.875$, where 15kW is the new inverter capacity, and 8 kW is the original inverter capacity

2.3.2 Design Alternative

After completing the earlier modified design, we decided to do another simulation based upon four alternative models, three of which did not require any extensive hardware additions to the solar house system. This was because we learned late into the design process that the solar inverters currently installed actually had the ability to operate at a capacity of 15 kW. Each of the two solar charge controller has a nominal rating of 5.8kW, and the Multiplus inverter has a rating of 10kW, while the Primo inverter has a rating of 5 kW.

Thus we designed four different models and simulated them using HelioScope. In the first setup, the system was limited to only 8 kW of inverter capacity. This represents the Solar House as it was in the SDME competition until now. In the second setup, the system has 15 kW of inverter capacity. This represents the Solar House if the limit were removed on the inverters presently installed. In the fourth setup, the system has 15 kW of inverter capacity, but the strings are reconfigured into a 40/20 panel arrangement in place of the current 35/25 arrangement. In the last setup, the system has 20 kW of inverter capacity. This represents the Solar House if the limit were removed on the inverters presently installed and an additional 5 kW inverter were to be installed.

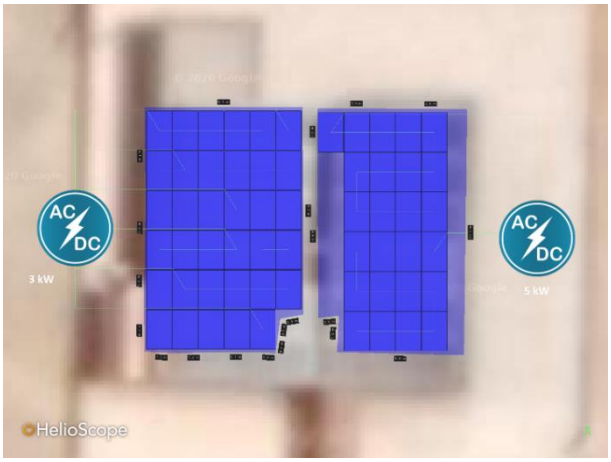

Figure 2.19 8kW Setup

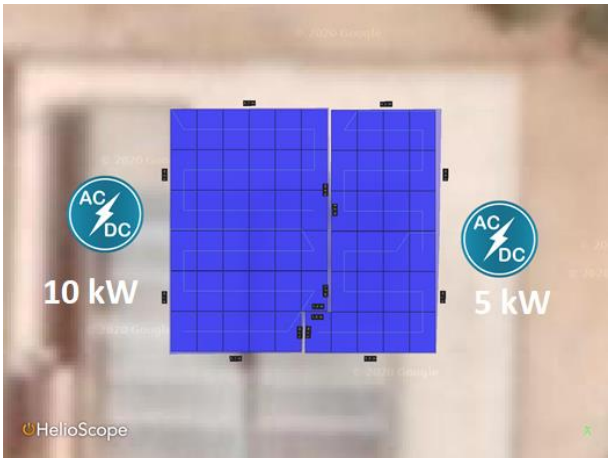

Figure 2.19 15kW 35/25 Setup

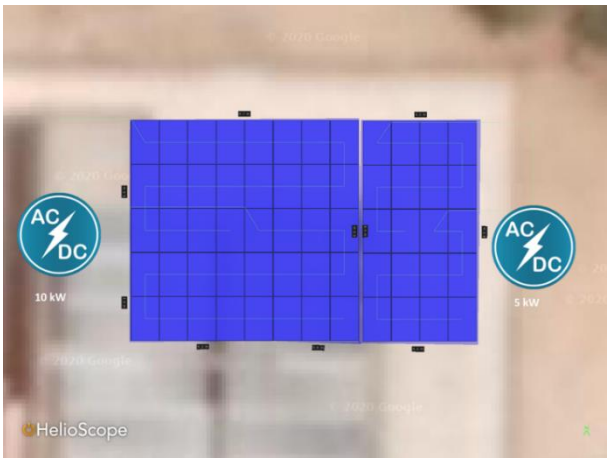

Figure 2.19 15kW 40/20 Setup

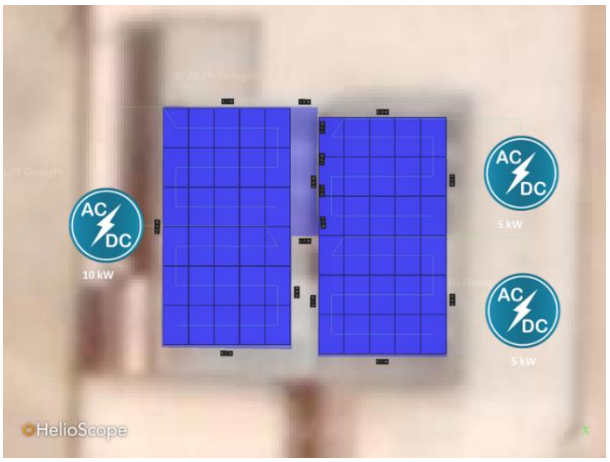

Figure 2.19 20kW Setup

2.3.2.1 Simulation Results

Table 7 Simulation energy yield comparison

Setup	8kW	15kW 35/25	15kW 40/20	20kW
Annual Energy Yield	23.08 MWh	30.37 MWh	30.43 MWh	30.40 MWh

Based upon the results seen in Table 7 and Figures 2.20 and Figure 2.21, we decided to forego the modified design which called for the addition of another inverter. It is clear from this data and the graphs that the system is not bottlenecked at the solar inverter stage. In fact, the 15kW and 20kW setups perform almost identicaly, with the alternative string arrangement setup performing similarly as well.

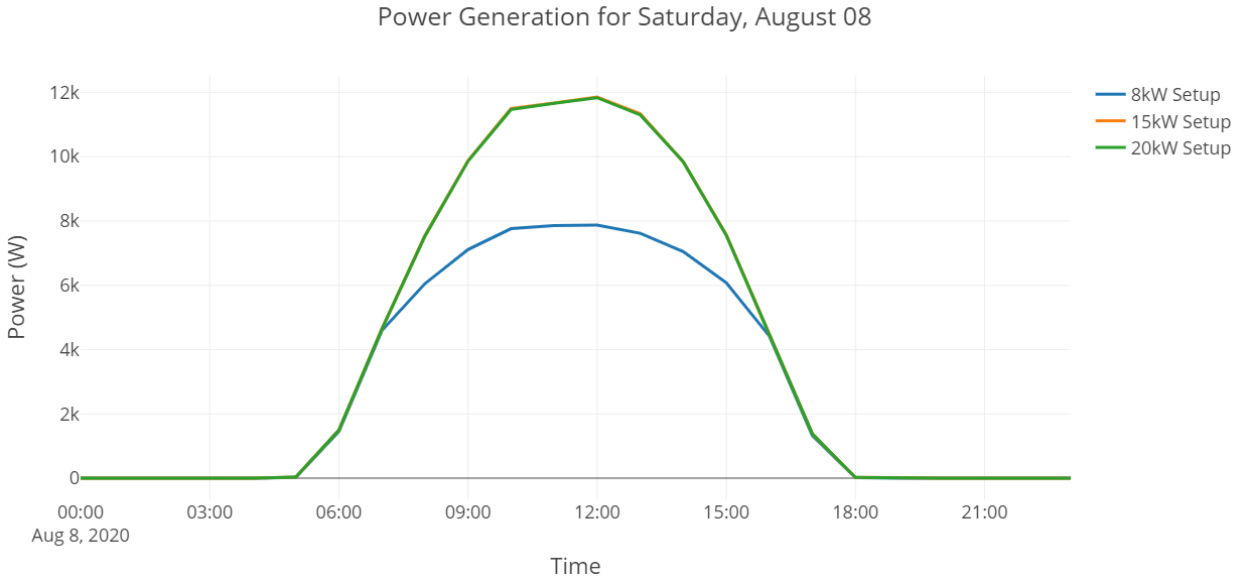

Figure 2.21 Simulation power generation for August 8

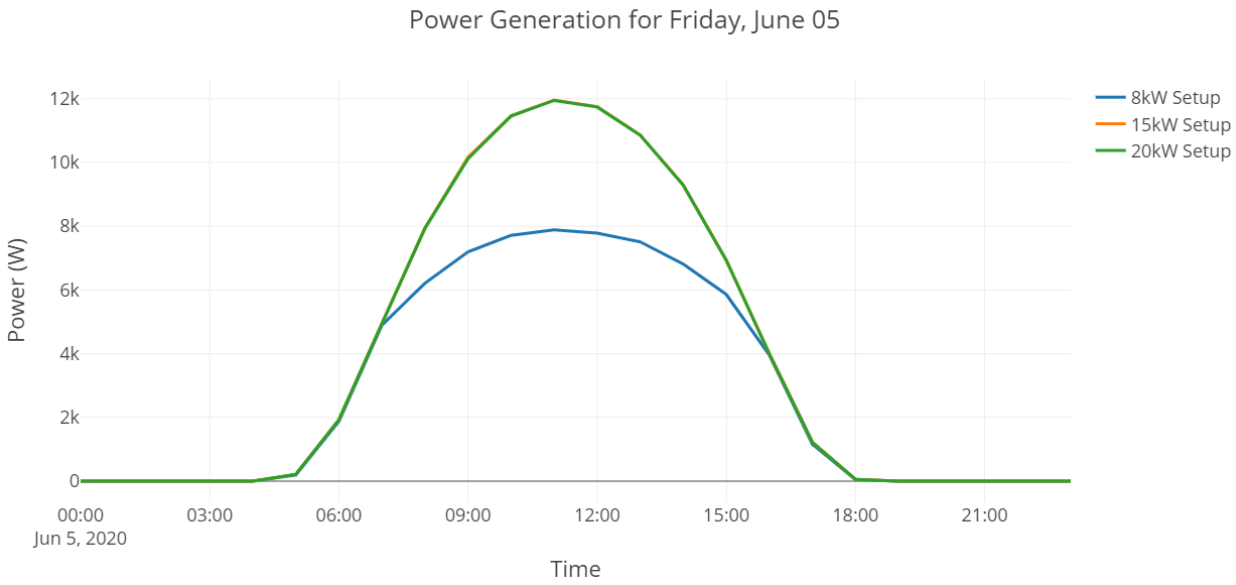

Figure 2.20 Simulation power generation for June 5th

2.3.3 Final design

Based upon our findings in the design and simulation phases, we decided that the best course of action would be as follows:

1- Test the current system and establish a baseline

2- Perform any repairs required

3- Reconfigure the system to follow the proposed 15 kW 35/25 setup

4- Remove all software limits imposed upon the system

5- Measure the final performance and verify with simulation data

If successful, this would result in maximizing the usage of the PV array, increasing the power generation of the system, and minimizing costs.

3 TESTING AND REPAIR

3.1 Assessing the State of the Current System

The initial visit to the Solar House gave us a chance to inspect the technical room[1] and the hardware installed therein. The technical room of the Solar House contains several important devices for the electrical, network, and security systems of the Solar House. The north wall of the room is dedicated to the PV system. Mounted there are the two solar charge controllers, the Victron Multiplus inverter, the Fronius Primo inverter, and the distribution panel. Affixed to the front of the distribution panel are the Color Control and the battery monitor. Figure 3.2 shows the north wall of the technical room.

The PV array string cables are collected at the west of the Solar House roof and enter the technical room via tubing in the north wall. These high voltage DC wires enter the distribution panel, shown in Figure 3.1, where each cable pair passes through a disconnect switch, a circuit breaker, and a surge arrestor before finally leaving the distribution panel.

Figure 3.1 The north wall of the technical room

Two strings are attached to the two MPPT inputs of the Fronius Primo solar inverter. The remaining two strings are each attached to the input of one of the two solar charge controllers. The output of the two solar charge controllers is then connected to the DC input of the Multiplus, while the output of the Primo inverter is connected to the AC input of the Multiplus. The battery system is further connected to the DC bus of the Multiplus, and finally a grid tie-in is connected to the AC bus of the Multiplus.

Thus, when the PV array is functioning and the power generation is sufficient to power the electrical loads of the Solar House, the Multiplus prioritizes first the AC loads of the house, then charging the batteries, and finally transfers excess power to the power grid. However, if the power generated by the array is too low to satisfy the loads, or during nighttime when there is no generation, the Multiplus draws power from the grid to power the Solar House.

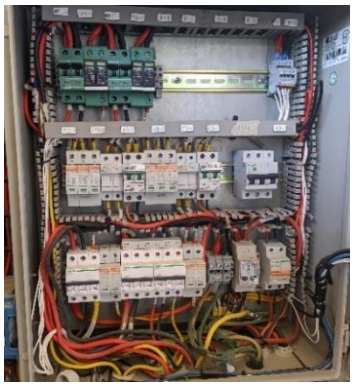

Figure 3.2 The main distribution panel

As currently configured, the ESS (energy storage system) is configured to only keep the batteries charged and not draw power from the battery system.

A cursory inspection of the solar inverters showed that both were operating, however the power generated was very low when considering the size of the array. This can be seen in Figure 3.3, which shows the display of the Color Control GX as seen during the first visit to the Solar House. Note that the Primo inverter was not connected to the Color Control at the time.

Figure 3.3 The Color Control GX display

[1] See Appendix for house layout

The ‘PV Charger’ reading is the combined output of both charge controllers, while the ‘Grid’ reading is the net power transfer to or from the grid. A positive value indicates power purchased from the grid, while a negative value indicates power sold to the grid.

The data collected by the Color Control was not being recorded, and so there was no historical data for the system. The system had not been used for any purpose after the competition, and thus data logging was not enabled. The only loads in the system were the devices in the technical room and small loads left on in the house (lights, water fixtures, utilities, etc.).

3.2 Testing the System

Before implementing any changes to the system, we had to measure the baseline performance, and ensure that the system was operating in the manner we expected it to. Thus, we had to test each device in the technical room, and inspect the PV array and all the wiring. We decided to begin in the technical room, as it was more accessible and any issues in the array or wiring would likely be seen in the device data.

We started at the Color Control monitor, which is a device that aggregates data from all connected devices and allows for data logging, and remote management of the system. It also serves as the hub for configuring the ESS. We noted that the device was not connected to the internet, and thus the remote logging and management capabilities were disabled. The device is capable of storing logs locally, however the internal storage is only allows for two days of local storage before logs are overwritten. This can be extended further via the use of a USB memory stick or a microSD memory card; however, neither option had been used to enable data logging [7].

The first step taken was to attempt to individually connect to the devices in the technical room and read their status. To achieve this, the Victron Connect application was used, this allowed a direct connection via Bluetooth to both solar charge controllers and the battery monitor. We first noted that the devices firmware was out of date; the firmware on the solar charge controllers was from February 2019[1], and had undergone several revisions since then that included fixed issues and added improvements. The two solar charge controllers were updated to the latest firmware release, and the battery monitor was similarly updated.

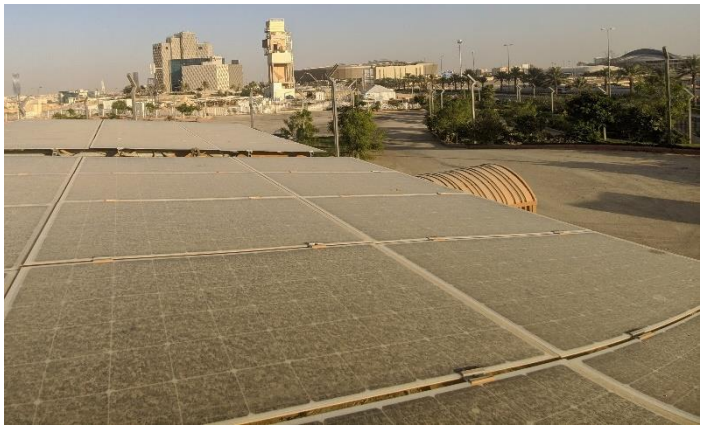

Figure 3.4 The PV array

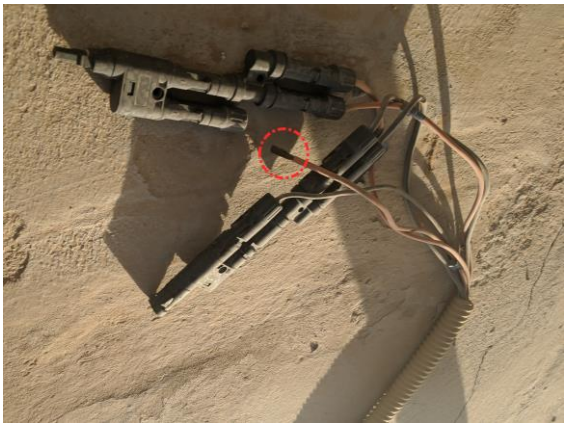

Figure 3.5 A disconnected string cable

The data from the solar charge controllers indicated that the second solar charge controller, henceforth MPPT2, was off due to insufficient PV voltage, and additionally it had generated only 302 kWh during its lifetime[1]. The first solar charge controller, henceforth MPPT1, had in contrast logged 6175 kWh of energy yield during its lifetime. This indicated that there was an issue with MPPT2, and that it likely had not been operating correctly for some time.

[1] The version installed was v1.39, released in February, 2019 as per VictronConnect changelog and beta releases

The max power generated during that day by MPPT1 was recorded as 2.6kW[1], whereas the 20 panels connected to MPPT1 had a rating of 290Wp each, leading us to expect a maximum of 5.8kWp. However, this data point was recorded in the month of November, when ambient temperatures and irradiance data indicates that we would be better served by using the NOCT rating of the panels, which is 210Wp. Thus, we would expect 20 panels to peak at 4.06kW, rather than the 2.6kW reported by MPPT1. This indicated an issue with either the configuration of MPPT1 or the PV array.

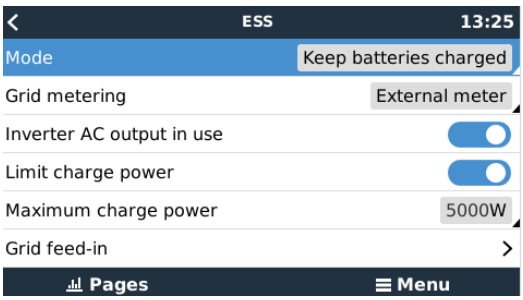

Figure 3.6 The ESS settings menu

Figure 3.7 The primo settings menu

We then turned our attention to the Fronius Primo solar inverter, which was not connected to the Color Control and thus its data was not being aggregated with the rest of the system. We connected it to the Color Control via a wireless network connection, and proceeded to verify its power generation log. It is relevant to note here that the Primo contains two MPPT ports, each capable of half its rated power generation. We noted an issue with the MPPT1 of the Primo, in that it was not producing power at all.

After securing proper safety equipment, we moved to inspect the PV array located atop the Solar House. We noted immediately the state of the modules; there was a large buildup of dust on the surface of the panels, and many of the MC4 connectors and string cables were exposed to the elements. We noted a frayed cable end near string 3, which is the string connected to MPPT2[2]. We measured the tilt angle[3] of the solar modules to be 7°, which agreed with the design specifications from the original project[4]. It should be noted that the optimum tilt angle for the current site is actually 26° [8]. This optimum angle is a yearly average, in the summer months the optimum angle is actually lower while in the winter months it is higher [9].

We attributed the low power generation of the system mainly to soiling. As can be seen in Figure 3.4, there was a large accumulation of dust on the panels.

Finally, there was the status of the limitations imposed upon the system during the competition. The Primo AC power generation was limited to 3 kW via the 'Manual Power Reduction' setting in the hidden menu accessible using an access code obtained from Fronius technical staff. Figure 3.7 shows this setting option. The other limiting in the system was imposed through the ESS settings in the Color Control, where it was set to limit charge power to 5 kW as shown in Figure 3.6.

[1] See Appendix for data.
[2] See Figure 3.11 for string diagram.
[3] See Appendix for detailed measurements
[4] See KSU Project Manual, page 40.

3.3 Soiling and Cleaning the Modules

In order to properly diagnose the system, we needed to eliminate the effect of soiling. Soiling, as noted before, can have a large detrimental effect on solar cell generation, by blocking the transmittance of light through the module glass to the solar cells enclosed within. Generally, this effect is not very large in climates with low rates of dust deposition [10]. In addition, it is mitigated in part by rain, where the solar modules, usually installed at an angle, are washed clean by rain to give a self-cleaning effect.

Unfortunately, the climate in Riyadh does not lend itself to this self-cleaning method. The rate of dust deposition in Riyadh is among the highest in the world [11] [12], and the composition of the dust particles is at the same time highly detrimental to the efficiency of the panels [13]. A study performed in Baghdad, found that one month of dust deposition led to a degradation of 18.74% in the efficiency of solar modules [14]. However, the rate of dust deposition in Riyadh is, on average, higher than in Baghdad [11]. Additionally, the Solar House modules have been exposed to dust in longer than one month, and thus the degradation should be even higher. In a study performed in Saudi Arabia, it was found that solar panel efficiency decreased by 40% after being exposed to dust deposition over a period of about six months [15]. Another study found that soiling could result in daily energy losses of over 20% [16].

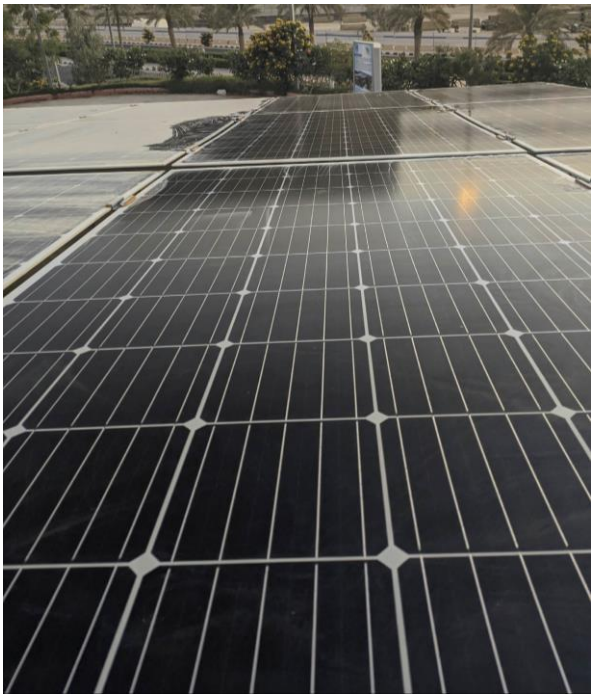

Figure 3.8 The solar modules during cleaning

We judged therefore that soiling was the main cause of the lower than expected power generation of the system. Taking as an example the case of the power generation figures recorded by MPPT1, we would expect a value around 4.06kW, whereas the device recorded a value of 2.6kW. This represents a difference of 35.9% percent, much higher than the standard losses in a PV system, and which agrees with the values of 18.74% and 40% set by [14] and [15] respectively. It should be noted also that the daily energy yield was similarly lower than expected.

Thus, we began the process of cleaning the modules, following established industry guidelines [17] [18] [19]. We chose to clean the modules before sunset, at a time when generation would be low so that module temperatures would not be high. Figure 3.8 highlights the contrast between the cleaned and uncleaned modules.

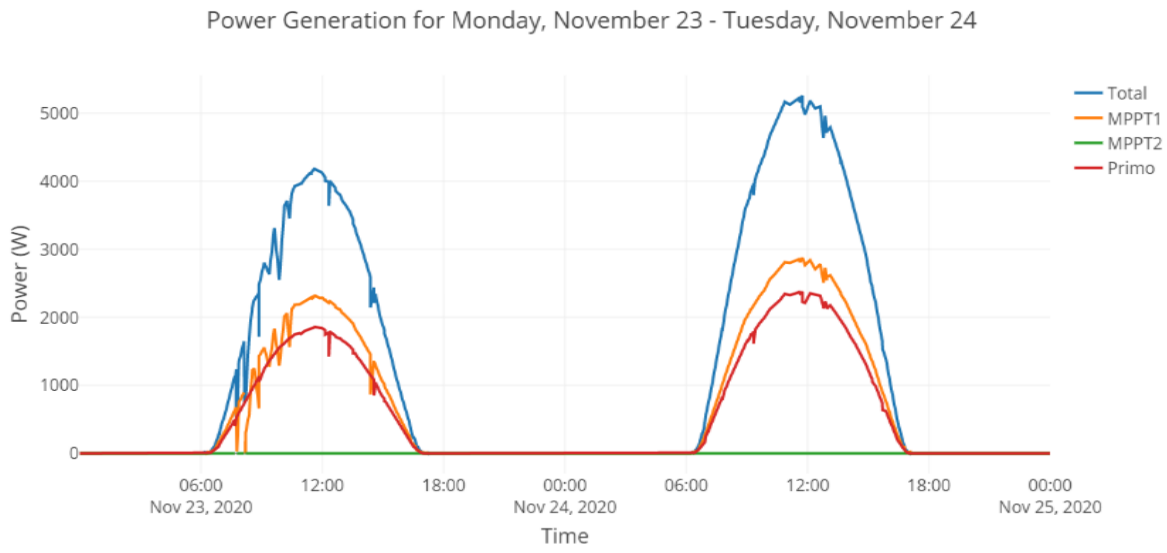

Figure 3.9 Power generation data before (left) and after (right) cleaning

Following the cleaning process, we noted a large increase in both peak power generation and the daily energy yield of the system. Figure 3.9 shows the power generation plot for the days before and after cleaning, while Table 1 shows the detailed data. Peak power generation the day before cleaning (November 23) was recorded as 4194W, while the day after cleaning (November 24) was recorded as at 5259W. This represents a substantial increase of 25.39% in peak power generation. Similarly, daily energy yield went from 25.37 kWh on November 23 to 33.59 kWh on November 24, which represents an increase of 32.40% in daily energy yield. The total energy yield for the 3 days before cleaning amounted to 78.48 kWh, whereas the total energy yield for the 3 days following cleaning was 100.91 kWh. This represents an increase of 28.58% in energy yield. Overall, it is clear that soiling had a large effect on the PV system of the Solar House, and was responsible for a large chunk of the lower than expected power generation.

We resorted to cleaning the modules a second time following a week of light rain showers, as it has been found low intensity rainfall can actually result in a decline in PV performance [20].

Table 8 Power generation and energy yield figures before and after cleaning

Day	**November 23**			**November 24**		
Device	**Peak Power (W)**	**Average Power (W)**	**Energy Yield (kWh)**	**Peak Power (W)**	**Average Power (W)**	**Energy Yield (kWh)**
MPPT1	2338.00	372.21	14.03	2873	578.58	18.32
Primo	1858.00	321.73	11.34	2374	472.60	15.27
Total	4194.00	687.06	25.37	5259	1050.82	33.59

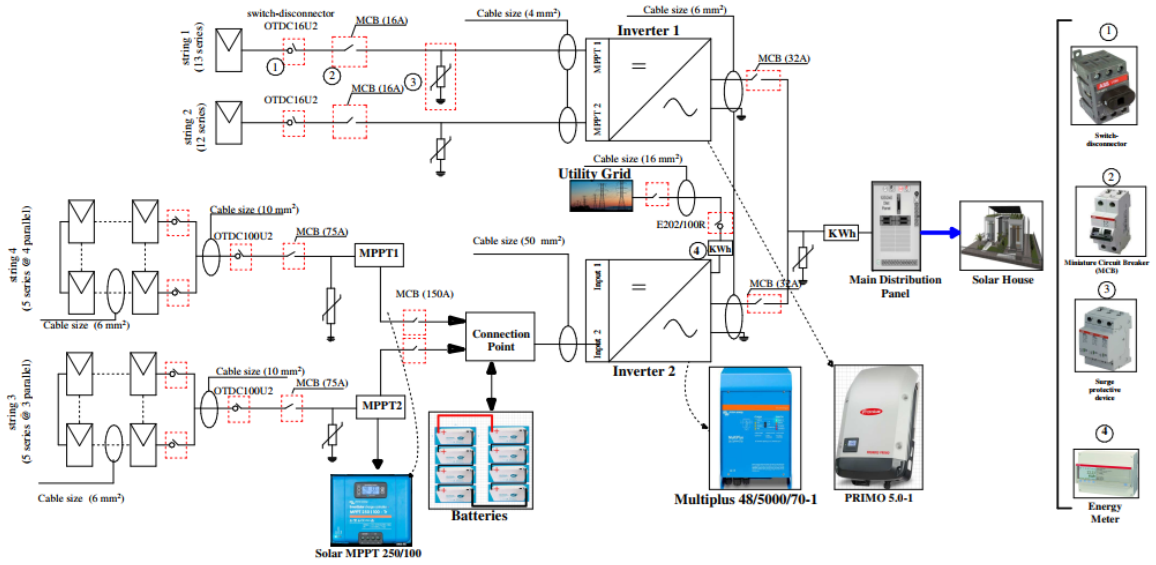

Figure 3.10 Line diagram of the system

3.4 Wiring Issues Found and Fixed

Having eliminated the issue of soiling from the system, we proceeded to further troubleshoot the state of MPPT1. As evident in Figure 3.10, MPPT1 is not functional, and reported a status of 'Insufficient PV Voltage'. This led us back to the wiring issue found earlier, seen in Figure 3.5. This cable is attached to String 3, which attaches to the input of MPPT1, thus we assumed it was the root cause of the issue.

We began by disconnected the system at the distribution panel, by flipping the disconnect switches and circuit breakers. We then used a digital multimeter to verify the open-circuit voltage of the cables adjacent to the broken end. The results of these measurements indicated that the strings were functioning normally. Afterwards, we proceeded to disconnect the panels upstream of the problem, in order to ensure that the naked cables would be safe to handle. After disconnecting all the upstream cables at the MC4 connectors, and ensuring that the cables were not live, we attached a new MC4 connector to the broken end.

We then reconnected the panels and measured the open-circuit voltage at the newly attached cable. This reading agreed with earlier readings of the functional cables.

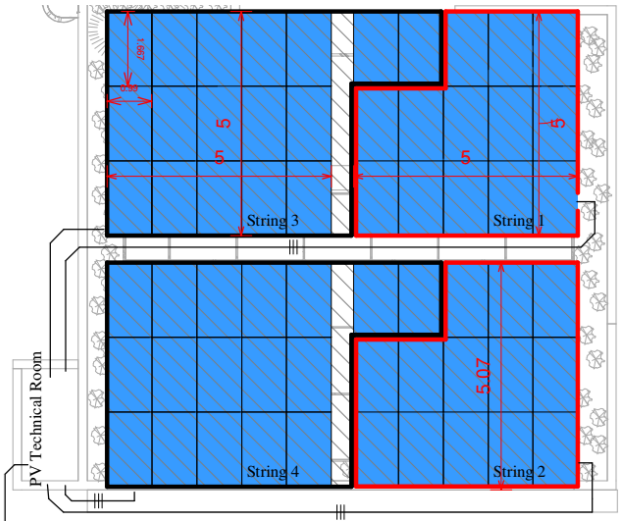

Figure 3.11 String layout atop the roof

We then followed String 3 to the collection point where all the string cables passed into the technical room, and found that it had not been connected to the collection point. We rectified this, and connected String 3 to the cable running into the technical room. Whilst connecting String 3, we noted an unconnected neutral wire.

Following this unconnected neutral wire to its origin, we found that it was one of the substrings making up String 4. We found that the MC4 Y-connector which was damaged, and could not be connected. We acquired a new MC4 Y-connector, and proceeded to remove the cables from the damaged connector. After connecting the wires using the new connector, we reconnected the panels and tested the open-circuit voltage of the wires, and the reading was reasonable.

We then reconnected the system and found that both MPPT1 and MPPT2 were functioning. Unfortunately, we could not immediately compare the newly collected data to the earlier data, as that week the weather was cloudy with light rain showers.

On the next clear day, we noted that although the Primo was connected to 25 solar panels in total, its output peaked at only 2.4 kW as can be seen in Figure 3.14. This was in contrast to MPPT1, which was connected to only 20 solar panels but had a peak power of 3.9 kW. Thus, we would expect the Primo to peak at 3 kW, due to the limit of 3 kW imposed via the 'Manual Power Reduction' setting.

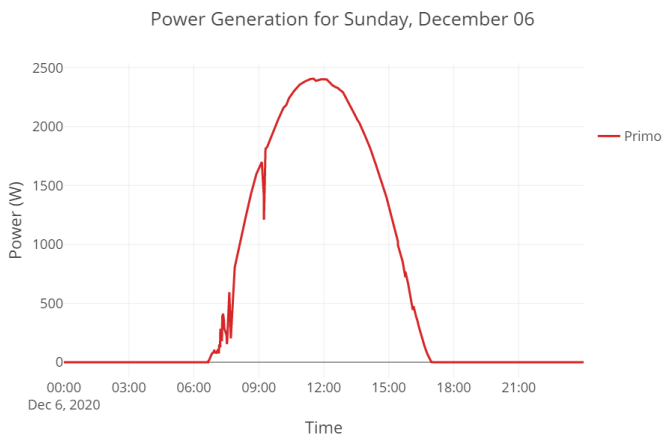

Figure 3.12 Primo power generation data

After looking into the detailed statistics in the Primo control panel, we found that the first internal MPPT in the primo, connected to String 1, was not functioning. We disconnected the system and measured the open-circuit voltage at the distribution panel. We found an abnormal reading compared to the reading for the second internal MPPT.

We moved to the PV array and measured the open-circuit voltage directly at the string, and found a normal reading. We diagnosed the issue to be between the collection point and the distribution panel. We reset the MC4 connectors at the collection point, and ensured that the circuit breakers and disconnect switch were functioning properly. After this, we measured the open-circuit voltage again at the distribution panel and found the same reading as that taken at the string.

Figure 3.13 String cables after repair

We think it is likely that there was a bad connection in one of the MC4 connectors at the collection point, and the issue had been hidden by the combination of the power limit set, and the effect of soiling causing it to be overlooked. After the issue was fixed, the Primo fully saturated the 3 kW power limit.
After ensuring that all the connections were correct, we secured the cables in a fashion to reduce any stress, and then covered the cables to protect them from the elements. This final arrangement of the cables can be seen in Figure 3.14.

Finally, we proceeded to remove the software limits set on the system, firstly by disabling the ESS power limit, and then by disabling the Primo power reduction setting.

4 DATA COLLECTION AND ANALYSIS

4.1 Setting up data collection and logging

Our goal was to analyze the live data from the system, and be able to compare that data to our simulation data. The Color Control GX has the ability to connect to an online portal called VRM (Victron Remote Management), where data would be uploaded and available for up to six months. The other option would be to utilize the local logging functionality of the Color Control and use a microSD card or flash drive to store the data, and then copy it to another device for processing. The first option was more attractive, as it would also enable remote management features such as a remote console, and alerts for system issues.

In order to setup data collection via the Color Control, we needed to connect all the devices to the Color Control, and then connect the Color Control to the internet. We used a 4G wireless router that had been used during the competition to connect the Primo to a wireless network. We then connected the Color Control to the same network using an Ethernet cable. The Color Control was then configured with the IP address of the Primo in order to connect the two. The Multiplus, solar charge controllers, and battery monitor were connected to the Color Control via direct cable connections as seen in Figure 4.1.

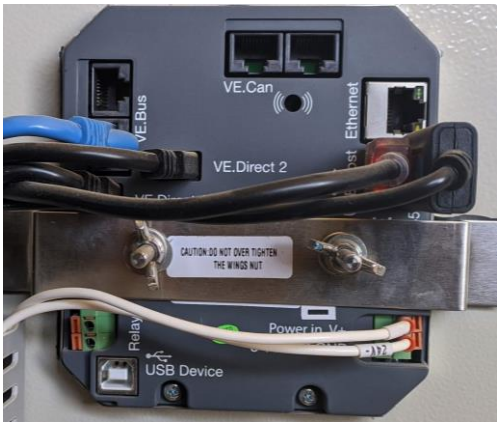

Figure 4.1 The back panel of the Color Control GX

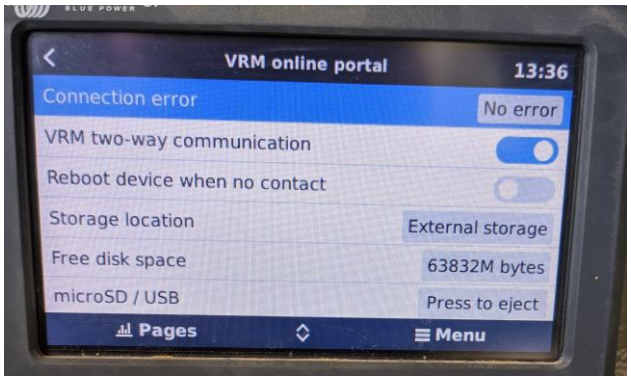

Figure 4.2 VRM portal settings on the Color Control

Next, we installed a new data SIM to the router for internet connectivity, and configured the VRM portal settings on the Color Control. We also installed a backup microSD card to log data in case of any connection issues.

This gave us access to the VRM online portal, where we could view live data from the system, access a remote console, and download archived system data. Figure 4.3 shows the VRM online portal.

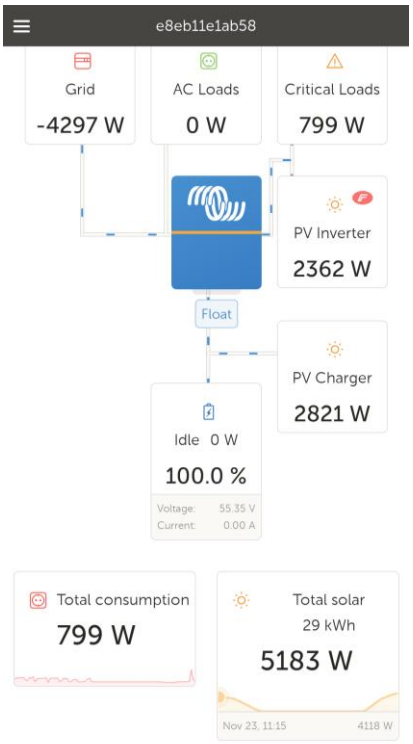

Figure 4.3 The VRM online portal

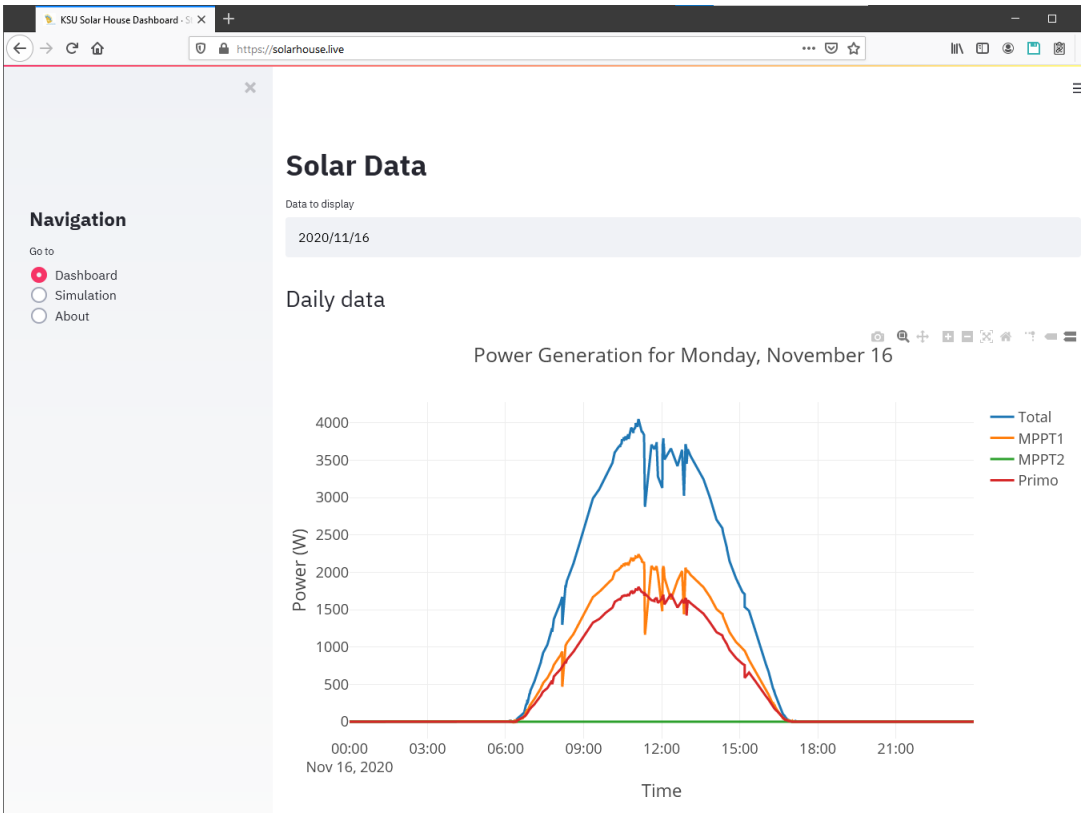

Figure 4.4 Main page of the online dashboard

4.2 Creating online dashboard

In order to access the VRM portal, a user name and password associated with the Solar House Victron account are required. Thus, in order to make viewing the data easier, and to allow us to highlight the data alongside our simulation models, we decided to create an online dashboard for the Solar House.

The dashboard would require access to the raw data collected from the Solar House. The VRM portal has a data export function, but this is unwieldy when trying to access large amounts of data. We looked therefore to the VRM API, which allows for easy programmatic access to site data. We made use of the python vrmapi library created by Victron in order to access the VRM API. We extended the library with a function to download the site data as a csv[1] file and created a program to parse the csv file into a pandas[2] dataframe.

Having the data in a usable format, we proceeded to create a dashboard using the Streamlit[3] framework. We wanted to highlight the daily performance figures of the solar house, as well as compare it to the simulation models. Figure 4.5 shows the main page of the online dashboard. This page allows for viewing the daily data for the system, as well as the individual device power statistics and energy yield.

Figure 4.4 shows the simulation page, where simulation data is plotted against the available solar house data, highlighting daily power statistics and cumulative energy yield.

The online dashboard also includes an about page, providing general information about the solar house and the project.

Once complete, the dashboard was a powerful tool in monitoring the solar house performance, and comparing it to the modeled data. Most of the graphs featured in this report, were generated using the online dashboard, such as Figure 4.6.

[1] Comma-separated values, a simple file format for storing data records.
[2] Pandas is a Python library for working with data sets.
[3] Streamlit is an open-source framework for creating data apps.

The dashboard can be accessed online at https://solarhouse.live

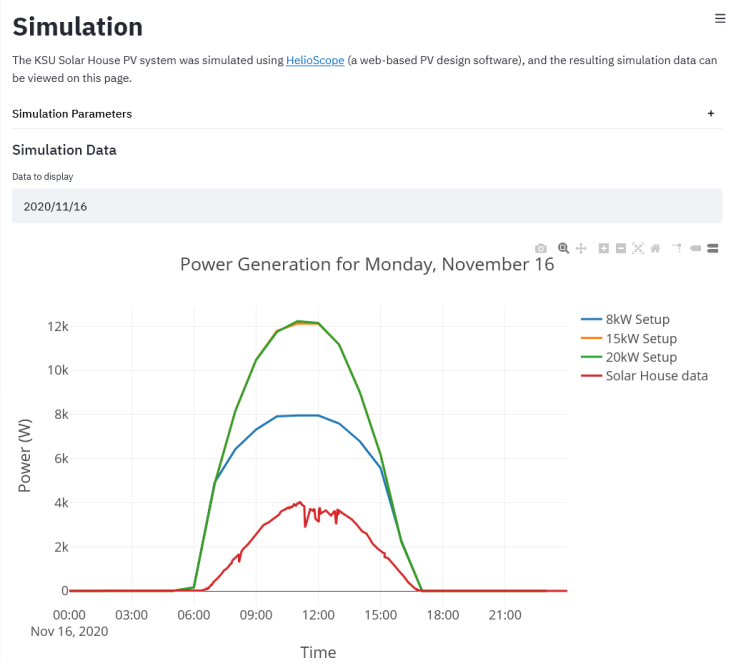

Figure 4.6 The simulation page of the online dashboard

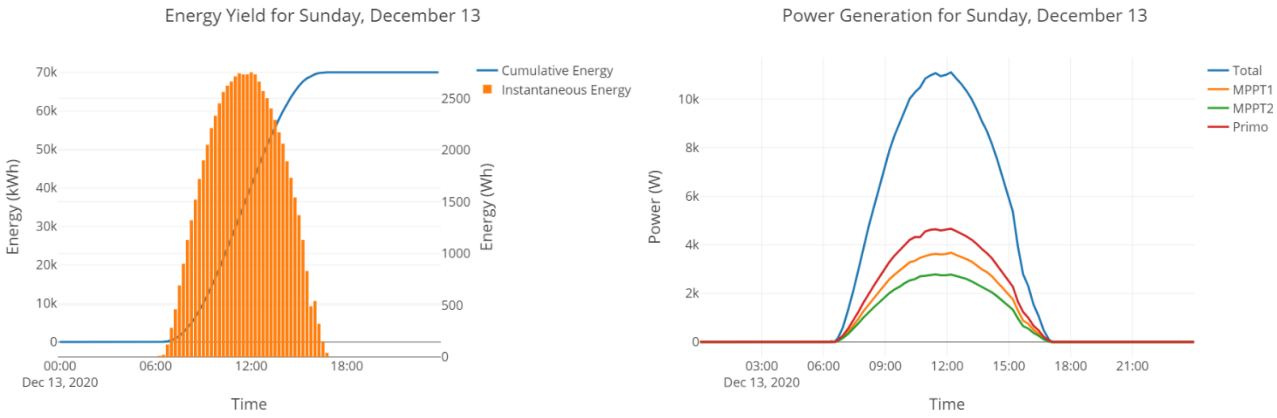

Figure 4.5 An example of two graphs generated using the online dashboard

4.3 Comparing to competition results

According to the SDME website[1], the solar house produced 550 kWh of energy over a period of ten days, from November 18 to November 28. This equates to an average daily energy yield of 55 kWh. Figure 4.8 shows the energy production graph from SDME. Figure 4.7 shows the energy production of the solar house over the period of December 11 to December 16, after the system had become fully operational. The total energy yield over this six-day period was 431.69 kWh, which represents an average daily energy yield of 71.83 kWh. This represents an increase of 30.6% in total energy yield over the competition results.

According to the Global Solar Atlas[2], the photovoltaic potential for Riyadh in mid-December is comparable to the photovoltaic potential for Dubai in late November.

Table 9 Competition results comparison

	Solar House at SDME	Solar House Unleashed	% Difference
Average Daily Energy Yield (kWh)	55	71.83	+30.6%

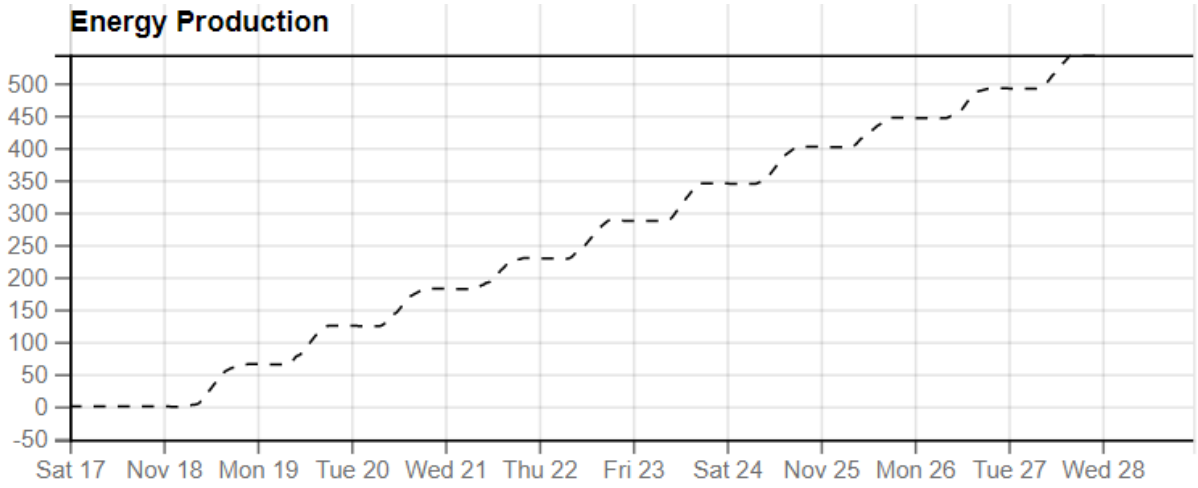

Figure 4.8 Energy yield of the solar house during SDME competition

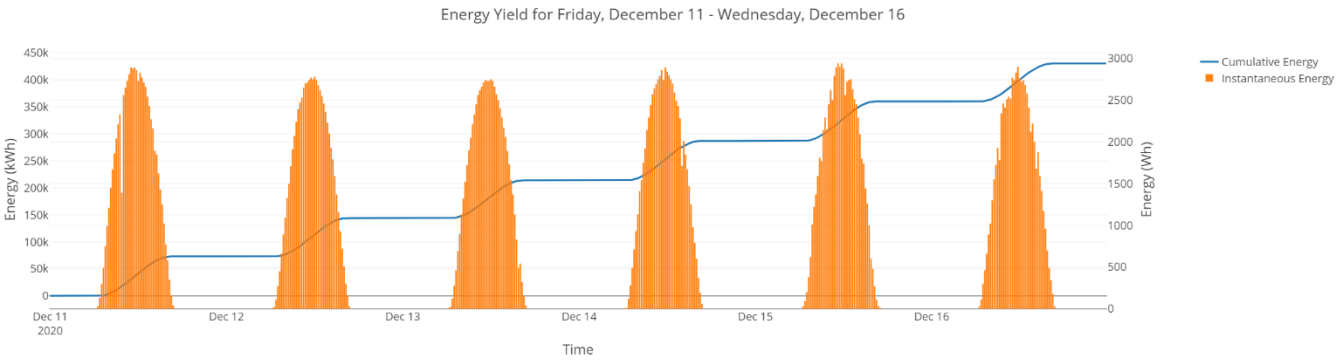

Figure 4.7 Graph of solar house energy yield over six-day period in December

[1] Accessed at https://sdme-contest.com/, energy consumption and production data viewed via the Weather Data subheading

[2] Based upon this page for Riyadh and this page for Dubai

4.4 Comparing to simulation data

Using the dashboard, we were able to compare the solar house data to the HelioScope simulation data. Figure 4.9 shows the three simulation models and the solar house data for the date of November 16. This is the first day we began data logging at the solar house, the modules were yet to be cleaned, and the wiring issues noted earlier had not yet been rectified. It is clear that the PV system of the solar house is underperforming by a significant amount, as the energy yields shown in Table 2 show clearly.

Table 10 Energy yield comparison for November 16

Data source	Energy Yield (kWh)	% Difference compared to solar house
20kW Setup	88.33	+265.9%
15kW Setup	88.288	+265.73%
8kW Setup	64.87	+168.72%
Solar House	24.14	+0%

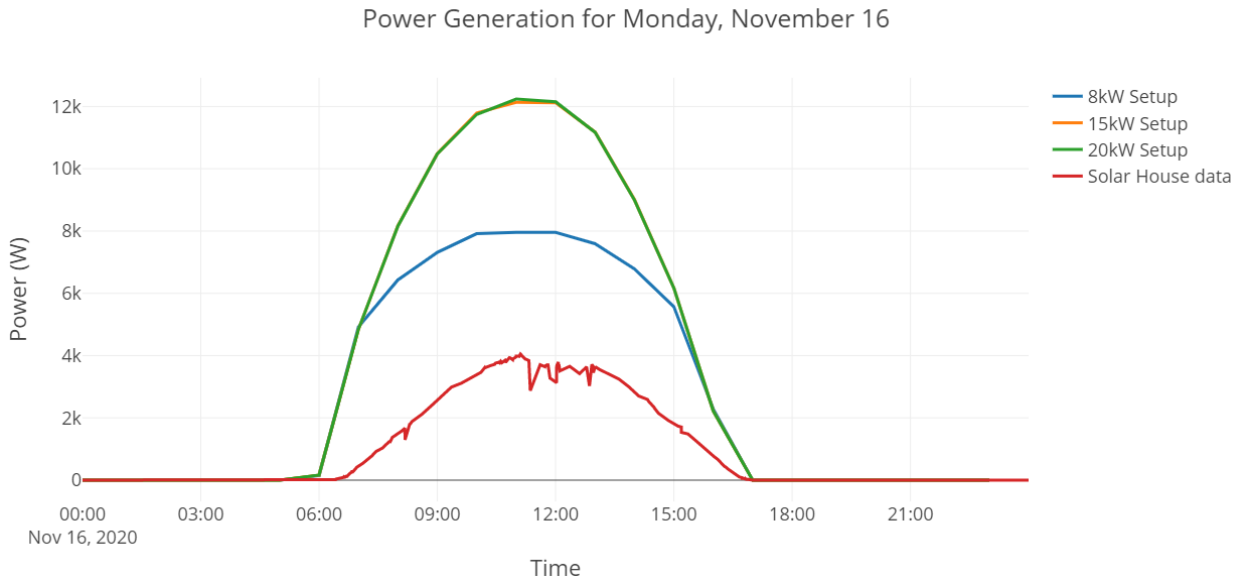

Figure 4.9 Power generation data comparing simulation to solar house for November 16

Following the cleaning of the modules, we saw a large increase in the power generation of the solar house and daily energy yield. Table 3 and Figure 4.10 show the energy yields and power plots respectively for the day of November 24, the first day after module cleaning. The difference in energy yield compared to the simulation models has shrunk significantly after cleaning, although the wiring issues had still not been fixed at this time.

Table 11 Energy yield comparison for November 24

Data source	Energy Yield (kWh)	% Difference compared to solar house
20kW Setup	92.77	+160.81%
15kW Setup	91.76	+157.97%
8kW Setup	65.99	+85.52%
Solar House	35.57	+0%

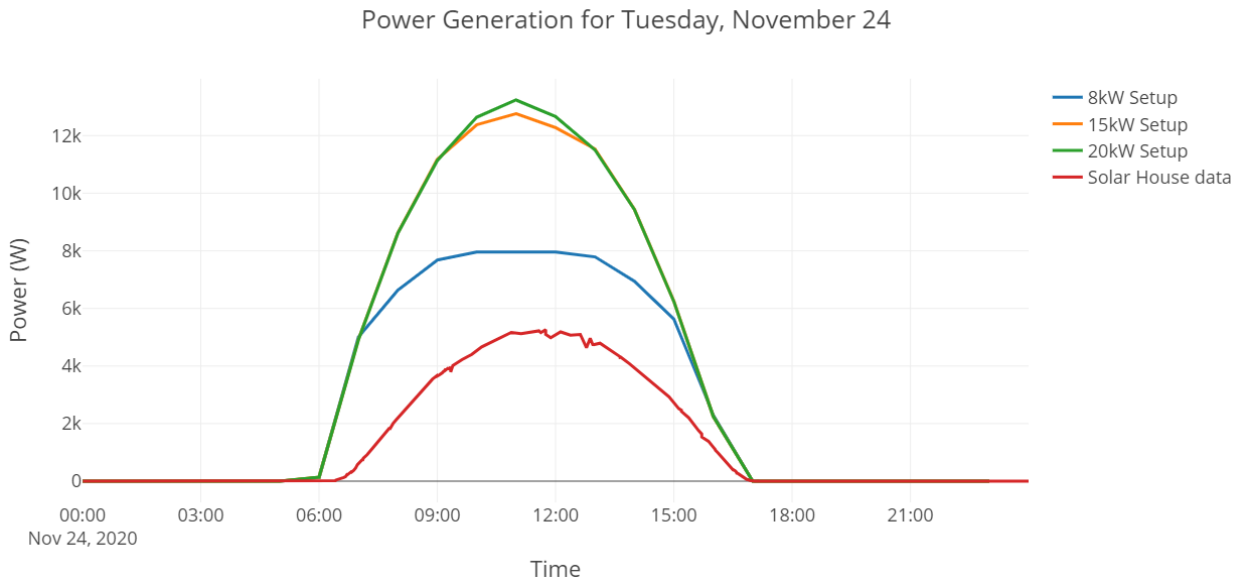

Figure 4.10 Power generation data comparing simulation to solar house for November 24

The next change in the solar house system occurred after fixing the issue found with MPPT2. Table 4 and Figure 4.11 show the relevant data from December 6. Note that the wiring issue with the internal MPPT of the Primo had not yet been fixed as of this data, and the house still has the 8kW limits imposed. This shows in the curve being clipped at 8kW. It is clear however that the solar house performance is very close to that of the 8kW simulation, with the deficit likely being caused by the Primo underperforming due to its wiring issue.

Table 12 Energy yield comparison for December 6

Data source	Energy Yield (kWh)	% Difference compared to solar house
20kW Setup	91.88	+46.86%
15kW Setup	90.98	+45.93%
8kW Setup	65.44	+13.79%
Solar House	57	+0%

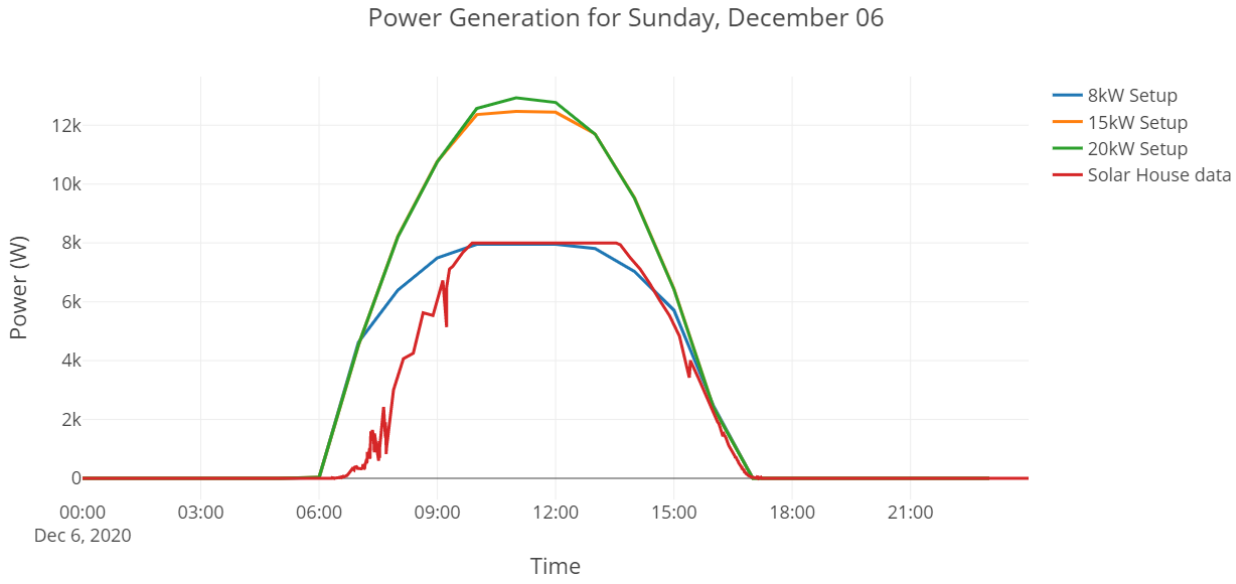

Figure 4.11 Power generation data comparing simulation to solar house for December 6

The next data point comes after fixing the issue with the first internal MPPT of the Primo inverter, and the data can be seen in Table 5 and Figure 4.12. At this point, the only issue in the solar house PV system is the software limitation.

Table 13 Energy yield comparison for December 11

Data source	Energy Yield (kWh)	% Difference compared to solar house
20kW Setup	86.91	+34.67%
15kW Setup	86.74	+34.48%
8kW Setup	63.6	+3.8%
Solar House	61.23	+0%

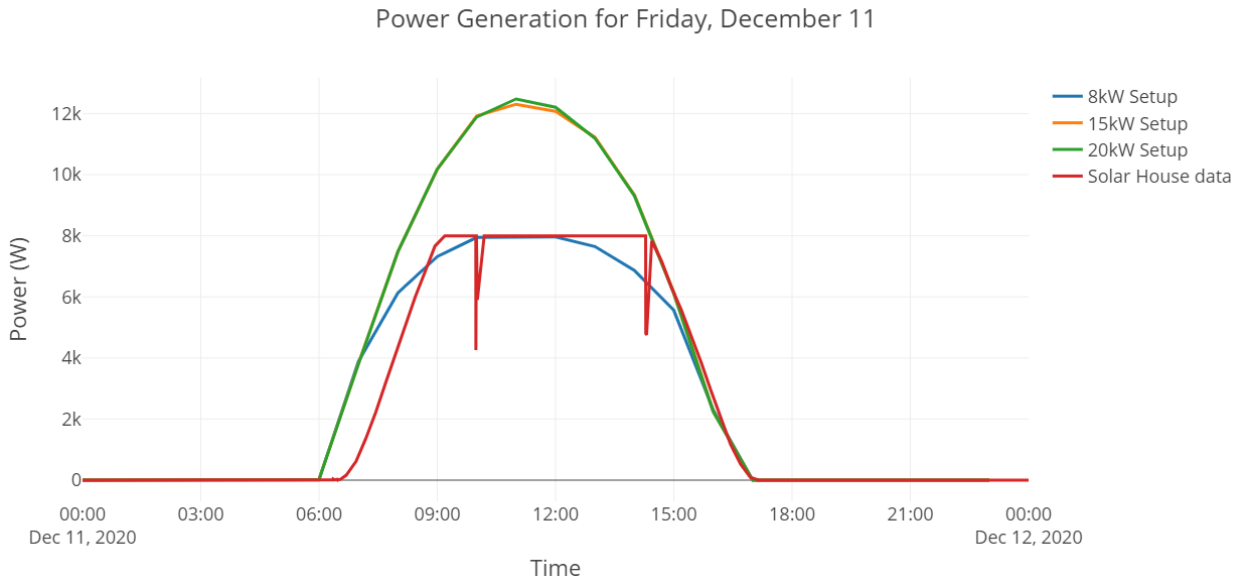

Figure 4.12 Power generation data comparing simulation to solar house for December 11

At this point, the difference between the 8kW simulation and the live solar house data are likely entirely covered by the combination of two factors: variability in daily irradiance from the weather data used to generate the simulation, and the simulation using a different more optimal tilt angle (22°) compared to the actual angle (7°) of the solar house modules.

The final data point is that of the house with all limitations removed and the system running at full potential. This data is shown in Table 6 and Figure 4.13. The house at this point has 15 kW of inverter capacity, and 18kWp of solar modules. Its performance should approach that of the 15kW simulation, albeit with the caveat that the tilt angle of the simulation differs from the tilt angle of the PV array at the solar house. The remainder of the difference in performance compared to the simulated model can be attributed again to variability in daily irradiance from the weather data used to generate the simulation.

Table 14 Energy yield comparison for December 13

Data source		Energy Yield (kWh)	% Difference compared to solar house
20kW Setup	75.54	+7.58%	
15kW Setup	75.68	+7.77%	
8kW Setup	58.33	-18.22%	
Solar House	70.02	+0%	

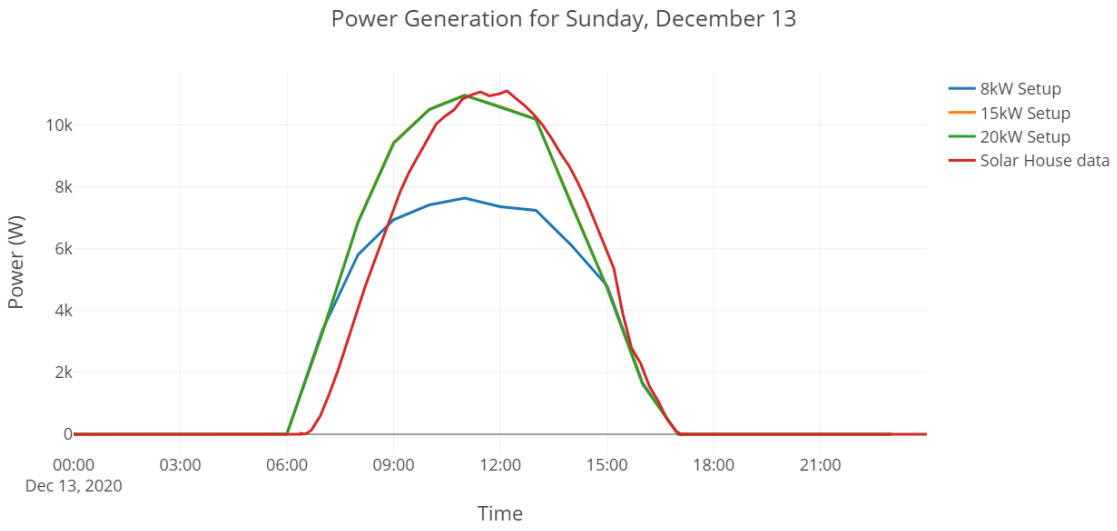

Figure 4.13 Power generation data comparing simulation to solar house for December 13

4.5 Discussion of Data

The solar house at its final state aligns closely with the 15kW simulation model.

The effect of tilt angle on energy yield is well known and has been quantified [21]. The tilt angle of the modules at the solar house is 7°, as opposed to the optimal annual angle of 26° [8]. The recommended method to increase generation would be to shift the tilt angle upward during the winter months and shift it downward during the summer months [9]. The choice of 7° for the solar house is interesting, as it does not appear to have been chosen to maximize production. The simulation models use the angle of 22°, which is closer to the optimal, and the most likely source of any discrepancies between the simulation data and the real world data.

The HelioScope simulation allows for the choice of either fixed-tilt or flush-mount modules. The main difference between these two configurations is in module cooling, where the fixed-tilt modules take up more space and suffer from shading, but have better ventilation allowing for lower module temperatures. The solar house array in effect is a hybrid of the two; the modules are placed in a configuration that eliminates inter-modules shading, but are not flush with the roof to which they are mounted. This means that thermal performance of the solar house PV array should be similar to a fixed-tilt array, while the shading performance should be similar to a fixed-tilt system. To test this hypothesis, we ran three additional simulations, all based upon the 15 kW model.

The tilt angle of all three models is set to 7°, as in the real solar house PV array. All three models have 15 kW of solar inverter capacity split into 35/25 strings. The first model has a fixed-tilt array. The second model has a flush-mount array. The third model has a flush-mount array with the temperature coefficients modified to be the same as the fixed-tilt model. Figure 4.14 shows the results of these simulations, averaged over one week of generation.

It is clear that the solar house data over performs compared to both the fixed-tilt and flush-mount models. This agrees with our hypothesis that the solar house PV array is a hybrid combining the best of each configuration. This is further reinforced by the results of the hybrid simulation model, termed flush temp on the graph. This is the model closest to the actual solar house data. This also explains why the solar house data performs so closely to the 15kW simulation with a 22° tilt angle, despite the large effect of tilt angle.

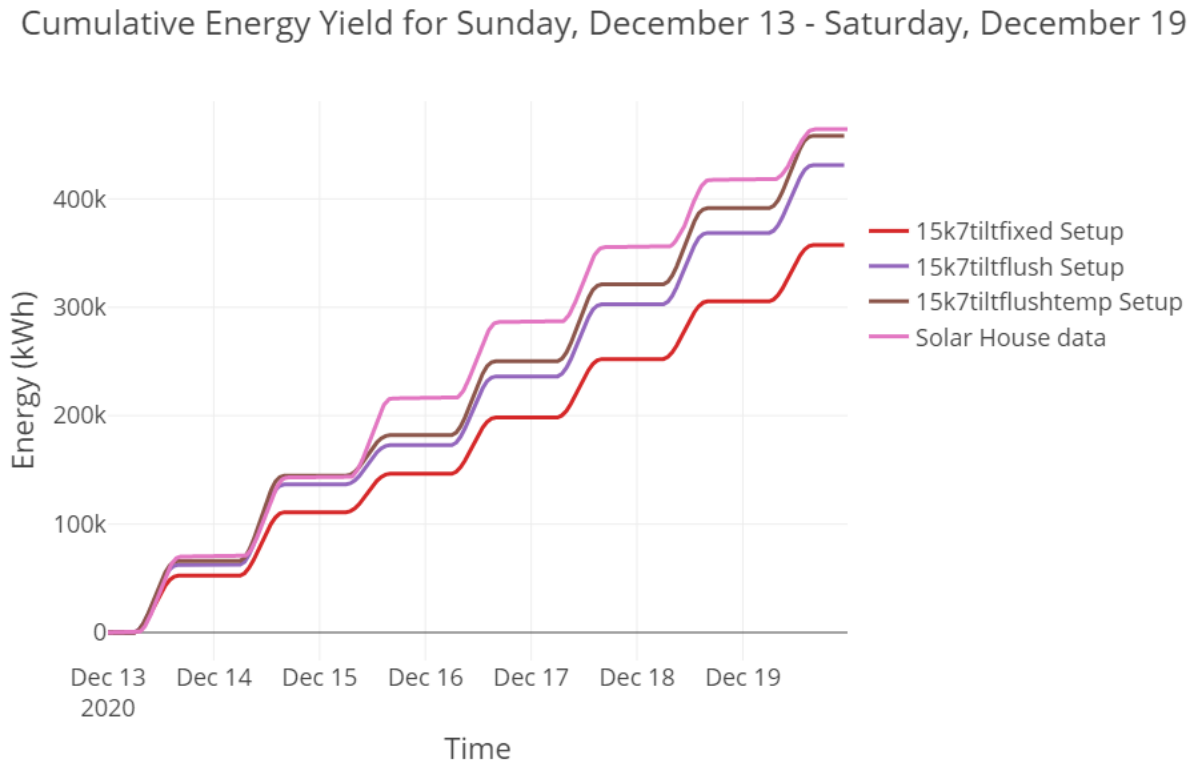

Figure 4.14 Different tilt model simulations

In reviewing the power production data, many sharp spikes, and steep drops can be observed. To understand this effect, it is helpful to think of solar modules as a very responsive sensor to sunlight. This is most noticeable on cloudy days or days with rainfall, a cloud passing over the modules can be seen as a steep drop in production, whereas a break in rainfall results in a sharp spike in production. This effect can be seen in Figure 4.15, where the spikes in generation correspond to the sky clearing up and vice versa vis-à-vis the drops in generation. Overall, we feel the data obtained indicates that the PV system is currently maximizing the potential of the PV array.

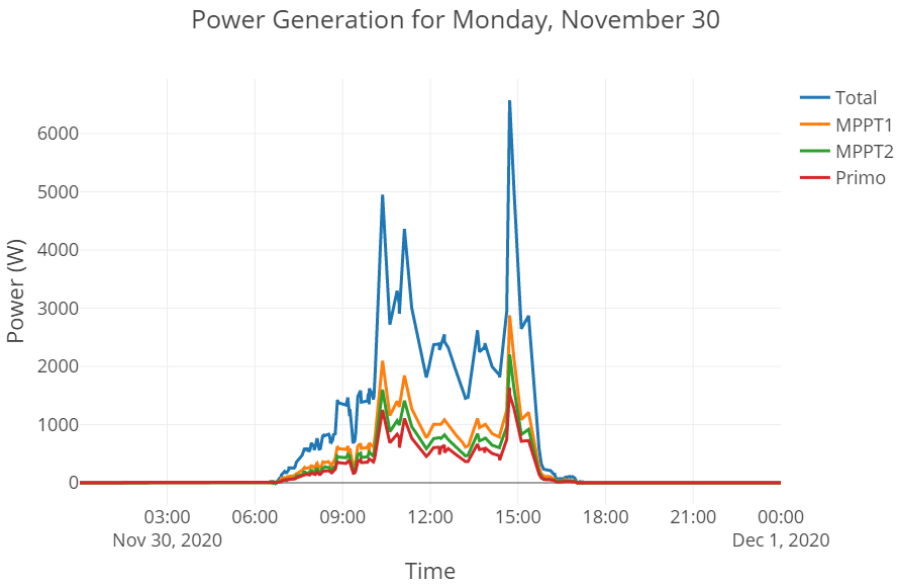

Figure 4.15 Power plot on a rainy day

5 CONCLUSION

5.1 Evaluating results achieved

The objectives of this project were as follows: to increase the generation of the PV system of the solar house, to maximize the usage of the entire PV array, and to establish remote monitoring and data collection. All while minimizing costs and modifications to the system.

The daily energy yield of the solar house PV system at the beginning of this project measured 24.15 kWh. The average daily energy yield of the solar house PV system at the SDME competition was 55 kWh. The average daily energy yield of the solar house PV system at the end of this project measured 71.83 kWh. Thus, we have achieved the goal of increasing the generation of the PV system of the solar house.

This value is very close to the peak potential of the solar house system according to simulation models, and thus we have maximized usage of the entire PV array.

The online dashboard we created and deployed allows for remote monitoring, data collection, and data analysis. The online dashboard is accessible online at https://solarhouse.live.

All of this was accomplished with minimal costs, namely only the cost of materials for repair and cleaning costs. Thus, this project has successfully achieved all the objectives laid out.

5.2 Potential uses of solar house

We suggest that the solar house be used for study of PV systems. During the course of our studies at KSU, we have taken a course on photovoltaics, which included a visit to a PV system not affiliated with the university. The solar house presents an opportunity to allow students access to a functional PV system built, managed, and maintained by students. We believe it would prove a very valuable resource for students and faculty alike.

Likewise, there is potential for using the solar house as a model for fully self-sufficient homes in a desert environment. Many models exist for other climates, but data for solar powered homes that deal with the difficulties of HVAC and soiling in a desert environment is relatively scarce. This could be achieved through opening the home to guided tours, and educational visits, as well as documenting in detail the challenges faced in construction and maintenance.

5.3 Future work

Possible avenues for further improvement to the solar house PV system are listed below:

- Adjusting the tilt angle of the modules to maximize generation, possibly with a tracking system.
- Better utilization of the battery storage system, which is currently unused.
- Expanding the PV array to the adjacent utilities and parking spaces nearby the solar house.
- Installing an automated cleaning system for the PV array.

6 BIBLIOGRAPHY

[1] M. A. Green, Solar Cells Operating Principles Technology and System Applications, Prentice-Hall, 1982.

[2] G. Masson and I. Kaizuka, "Trends in Photovoltaic Applications," International Energy Agency, Photovoltaic Power Systems Programme, 2019.

[3] M. F. J. T. A. Metz, "International Technology Roadmap for Photovoltaics (ITRPV) 8th edition," in *PV Manufacturing in Europe Conference*, Brussels, 2017.

[4] R. G. Ross Jr and M. I. Smokler, "Flat-Plate Solar Array Project Final Report Volume VI: Engineering Sciences and Reliability," Jet Propulsion Laboratory, California Institute of Technology, 1986.

[5] R. Messenger and H. Abtahi, Photovoltaic Systems Engineering, Fourth ed., CRC Press, 2017.

[6] Endecon Engineering, "A GUIDE TO PHOTOVOLTAIC (PV) SYSTEM DESIGN AND INSTALLATION," California Energy Commission, 2001.

[7] Victron Energy, "Color Control GX manual [Victron Energy]," [Online]. Available: https://www.victronenergy.com/live/ccgx:start. [Accessed 12 December 2020].

[8] Global Solar Atlas, "Global Solar Atlas," 2020. [Online]. Available: https://globalsolaratlas.info/map?s=24.732556,46.61843,10&pv=small,180,7,18. [Accessed 14 December 2020].

[9] M. M. El-Kassaby, "Monthly and daily optimum tilt angle for south facing solar collectors; theoretical model, experimental and empirical correlations," *Solar & Wind Technology,* vol. 5, no. 6, pp. 589-596, 1988.

[10] T. Sarver, A. Al-Qaraghuli and L. L. Kazmerski, "A comprehensive review of the impact of dust on the use of solar energy: History, investigations, results, literature, and mitigation approaches," *Renewable and Sustainable Energy Reviews,* vol. 22, pp. 698-733, 2013.

[11] A. Modaihsh, A. Ghoneim, F. Al-Barakah, M. Mahjoub and M. Nadim, "Characterizations of Deposited Dust Fallout in Riyadh City, Saudi Arabia," *Polish Journal of Environmental Studies,* vol. 26, no. 4, pp. 1599-1605, 2017.

[12] A. S. Modaihsh and M. O. Mahjoub, "Falling Dust Characteristics in Riyadh City, Saudi Arabia," *APCBEE Procedia,* vol. 5, pp. 50-58, 2013.

[13] J. Kaldellis and M. Kapsali, "Simulating the dust effect on the energy performance of photovoltaic generators based on experimental measurements," *Energy,* vol. 36, no. 8, pp. 5154-5161, 2011.

[14] M. Saidan, A. G. Albaali, E. Alasis and J. K. Kaldellis, "Experimental study on the effect of dust deposition on solar photovoltaic panels in desert environment," *Renewable Energy,* vol. 92, pp. 499-505, 2016.

[15] B. Nimmo and S. A. M. Said, "Effects of dust on the performance of thermal and photovoltaic flat plate collectors in Saudi Arabia - Preliminary results," *Alternative energy sources II*, vol. 1, pp. 145-152, 1981.

[16] J. Zorrilla-Casanova, M. Piliougine, J. Carretero, P. Bernaola, P. Carpena, L. Mora-López and M. Sidrach-de-Cardona, "Analysis of dust losses in photovoltaic modules," in *World Renewable Energy Congress 2011*, Linköping, Sweden, 2011.

[17] M. R. Maghami, H. Hizam, C. Gomes, M. A. Radzi, M. I. Rezadad and S. Hajighorbani, "Power loss due to soiling on solar panel: A review," *Renewable and Sustainable Energy Reviews,*, vol. 59, pp. 1307-1316, 2016.

[18] The Renewable Energy Hub, "How to clean Solar Panels | The Renewable Energy Hub," 2020. [Online]. Available: https://www.renewableenergyhub.co.uk/main/solar-panels/solar-panel-cleaning/. [Accessed 20 November 2020].

[19] First Solar, "FS-Series PV Module Cleaning Guidelines - First Solar," 2017. [Online]. Available: http://www.firstsolar.com/-/media/First-Solar/Technical-Documents/Series-4-Application-Note/Module-Cleaning-Guidelines.ashx?la=en. [Accessed 20 November 2020].

[20] A. Kimber, L. Mitchell, H. Wenger and S. Nogradi, "The Effect of Soiling on Large Grid-Connected Photovoltaic Systems in California and the Southwest Region of the United States," in *2006 IEEE 4th World Conference on Photovoltaic Energy Conference*, Waikoloa, HI, 2006.

[21] E. Asl-Soleimani, S. Farhangi and M. Zabihi, "The effect of tilt angle, air pollution on performance of photovoltaic systems in Tehran," *Renewable Energy*, vol. 24, no. 3-4, pp. 459-468, 2001.

[22] R. G. Ross Jr, "Flat-Plate Photovoltaic Array Design Optimization," in *14th IEEE Photovoltaic Specialists Conference*, San Diego, 1980.

[23] M. Seyedmahmoudian, B. Horan, R. Rahmani, A. Maung Than Oo and A. Stojcevski, "Efficient Photovoltaic System Maximum Power Point Tracking Using a New Technique," *Energies*, 2016.

[24] E. Zell, S. Gasim, S. Wilcox, S. Katamoura, T. Stoffel, H. Shibli, J. Engel-Cox and M. Al Subie, "Assessment of solar radiation resources in Saudi Arabia," *Solar Energy*, pp. 422-438, 2015.

7 APPENDICES

7.1.1 Definitions

AM: Air mass. Defined as $\frac{1}{\cos(\theta)}$ where θ is the zenith angle. The air mass is 1 when the sun is directly overhead.

Ampacity: Refers to "ampere capacity", the maximum current, in amperes, that a conductor can carry continuously under the conditions of use without exceeding its temperature rating.

FF: Fill Factor. It is defined as $\frac{V_{mp} \times I\_mp}{V_{oc} \times I\_sc}$ and it determines the maximum power output of a solar cell. A higher fill factor is desirable.

I_{mp}: Max power current. It is the current at the maximum power point.

I_{sc}: Short circuit current. It is the current through the solar cell when the solar cell is short-circuited.

MCB: Miniature Circuit Breaker, a type of circuit breaker that is rated for less than 100 amperes.

MPPT: Maximum power point tracking. MPPT allows the PV modules to operate at the maximum power point in the IV curve, and usually operates in a certain voltage range only.

NOCT: Nominal operating cell temperature. The NOCT is the temperature the cells will reach when operated at open circuit in an ambient temperature of 20°C at AM 1.5 irradiance conditions, G = 0.8 kW/m2, and a wind speed less than 1 m/s.

PV: Photovoltaic. The photovoltaic effect is the basis of operation upon which solar cells are built.

Soiling: Soiling refers to the accumulation of dirt, dust, and other particles on the surface of a solar module, leading to losses in power generation [4]

Solar Charge Controller: A device that acts as a connection point between a PV array and other components. Usually it integrates some kind of MPPT and battery charging functionality. The input and output are both DC, although the input is usually the variable DC produced by a PV array and the output is fixed voltage DC.

Solar Inverter: A device that converts direct current produced by a PV array in alternating current usable in households or ready for grid tie.

Solar Module: Also called a solar panel, a solar module is made up of many solar cells connected together and enclosed by some kind of encapsulation.

STC: Standard testing conditions. Refers to ambient temperature of 25°C at AM 1.5 irradiance conditions, G = 1 kW/m2.
String: A series-connected set of solar modules.

V_{mp}: Max power voltage. It is the voltage at the maximum power point.

V_{oc}: Open circuit voltage. It is the maximum voltage available from the solar cell, when the current is zero.

Wp: This refers to the nominal power of a PV device. This is usually the nameplate rating, and differs significantly from the capacity under real world conditions.

7.1.2 Additional Figures

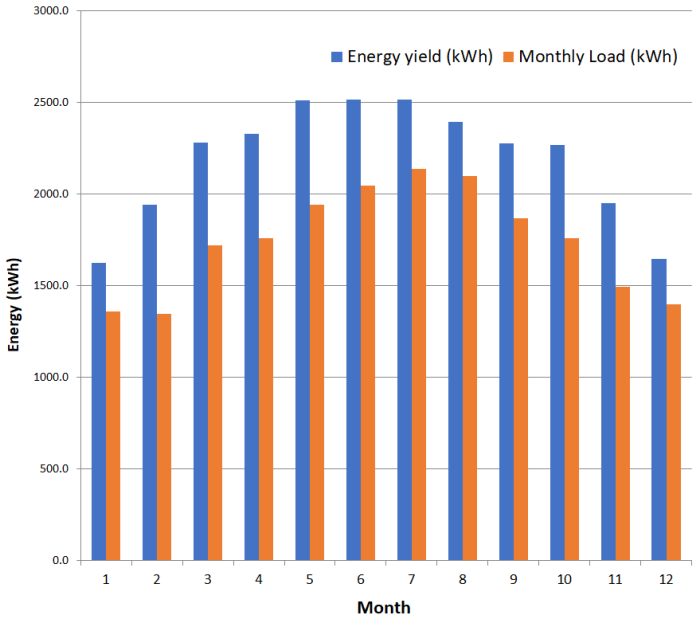

Figure 7.2 Original design simulation annual energy yield

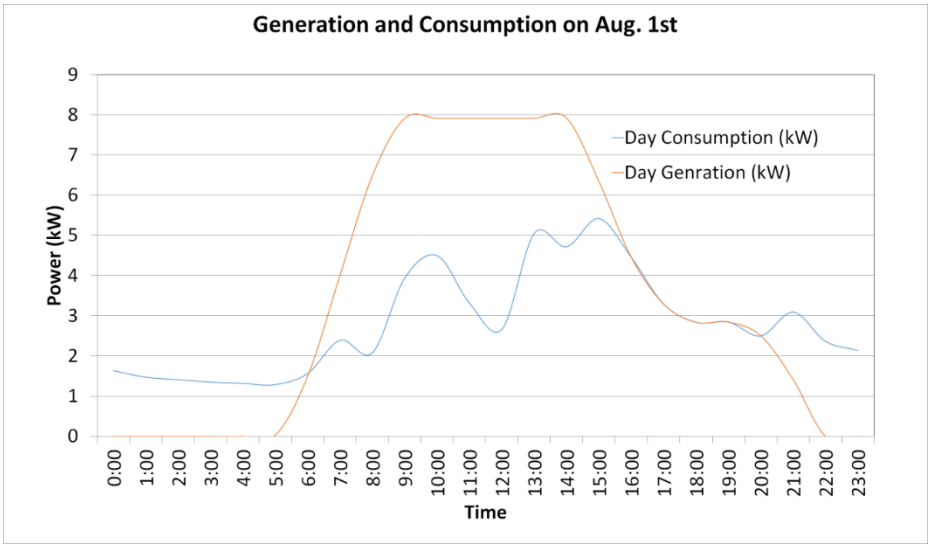

Figure 7.1 Original design simulation consumption and generation for Aug. 1st

Figure 7.4 Temperature reading of the modules during operation

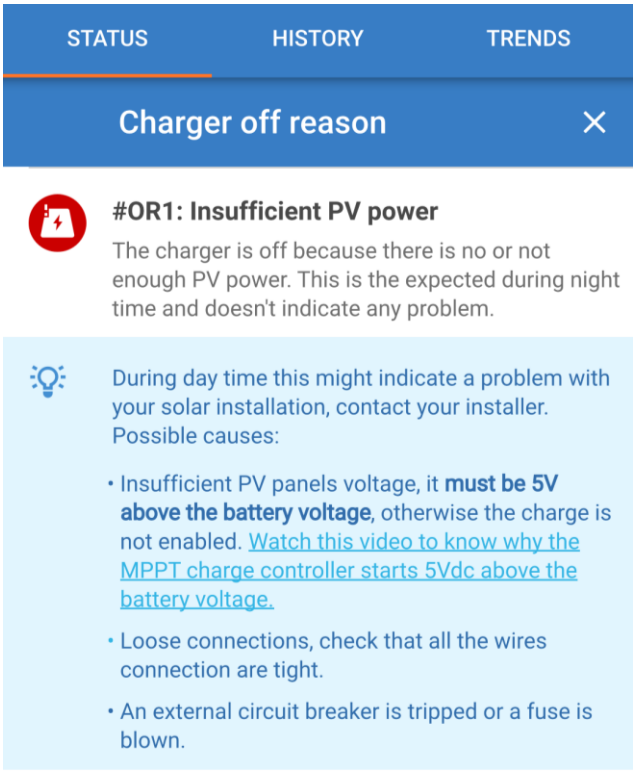

Figure 7.3 Screenshot of the issue reported by MPPT2

Figure 7.5 Picture showing the shading provided by the PV array

Figure 7.8 Updating the firmware of the MPPT

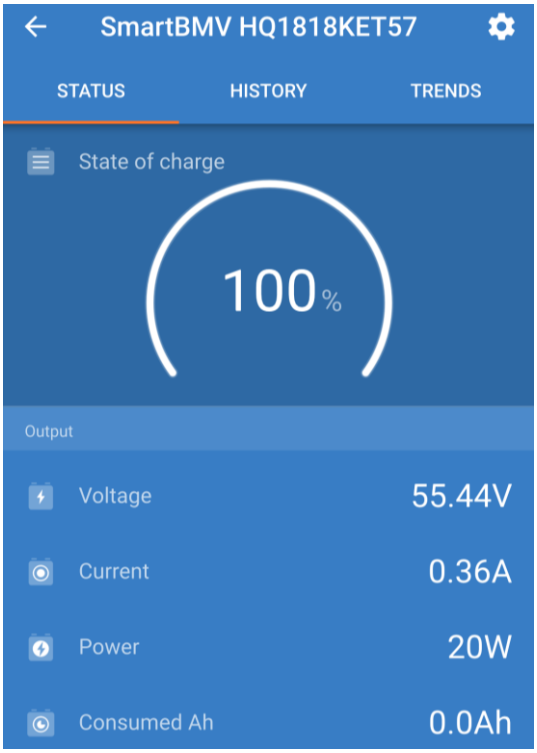

Figure 7.7 Status page of battery monitor

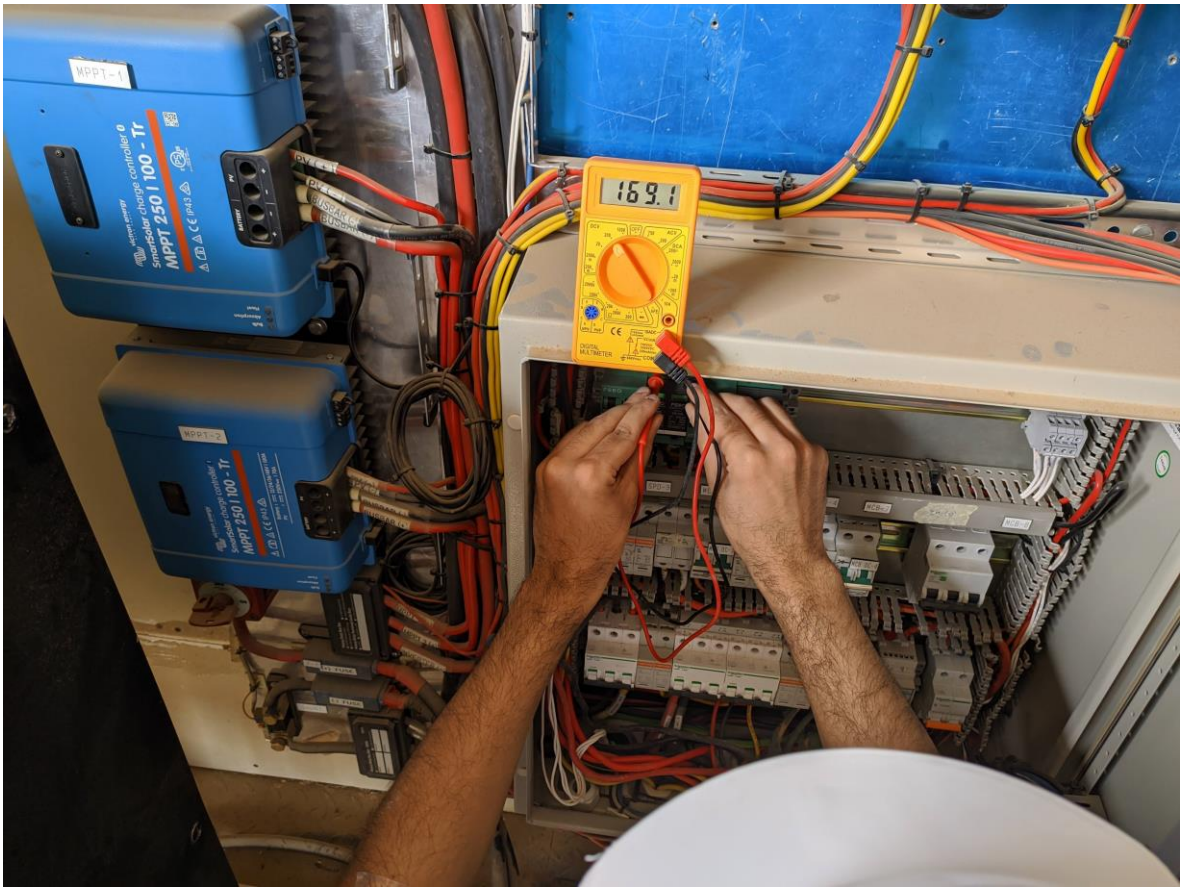

Figure 7.6 Taking measurements of the string voltages at the distribution panel

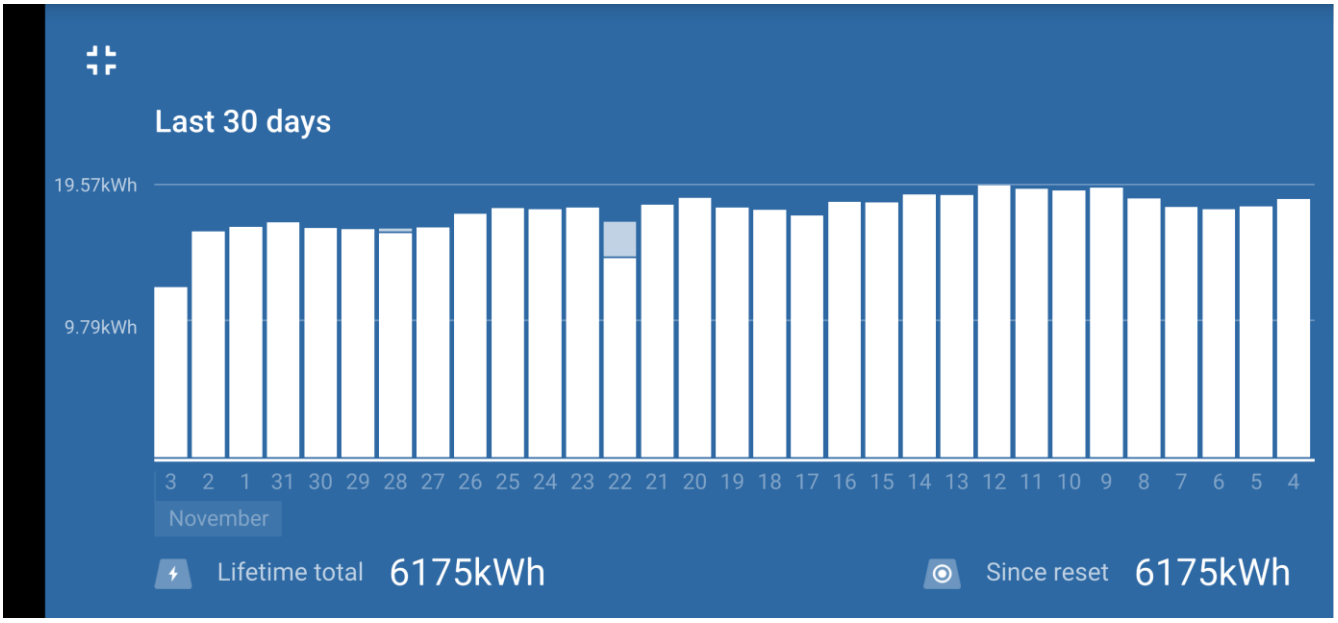

Figure 7.9 Lifetime total and log of MPPT1

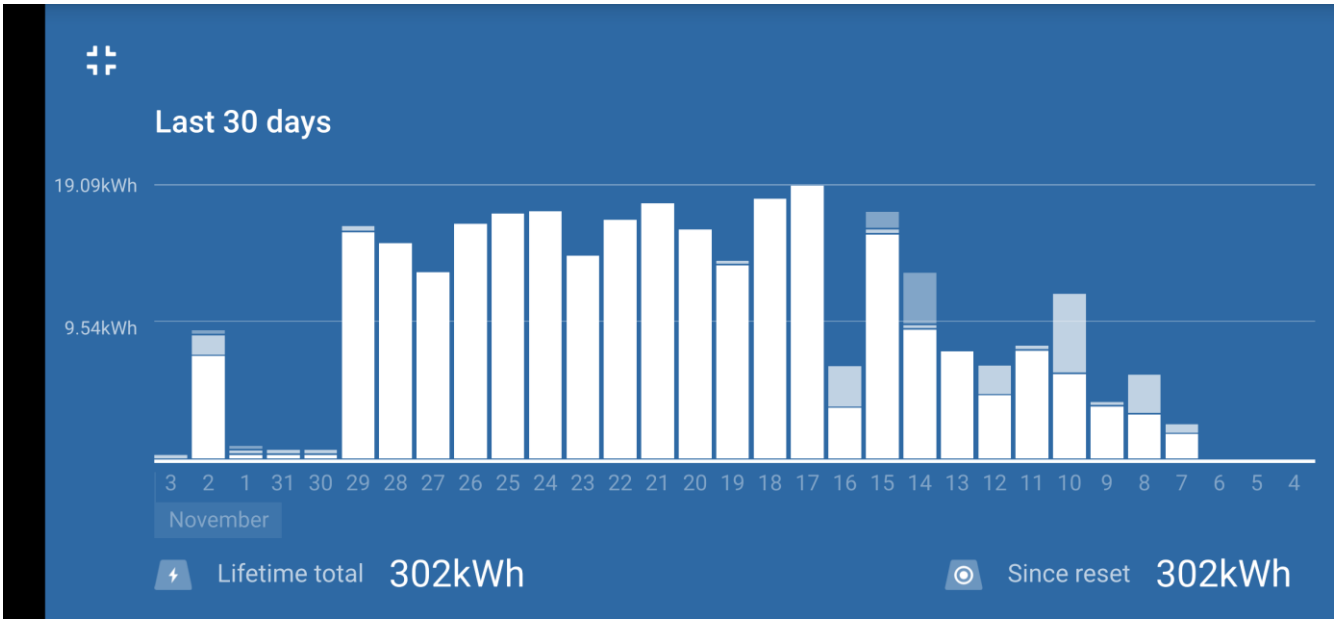

Figure 7.10 Lifetime total and log of MPPT2

Wiring Zones

Description	Combiner Poles	String Size
Wiring Zone	12	5-5
Wiring Zone 2	12	12-13

Field Segments

Description	Racking	Orientation	Tilt	Azimuth	Intrarow Spacing	Frame Size	Frames	Modules	Power
35 Modules	Flush Mount	Portrait (Vertical)	23°	180°	0.0 m	1x1	35	35	10.2 kW
25 Modules	Flush Mount	Portrait (Vertical)	23°	180°	0.0 m	1x1	25	25	7.25 kW

Figure 7.13 8kW Setup simulation parameters

Wiring Zones

Description	Combiner Poles	String Size
Wiring Zone	12	8-23
Wiring Zone 2	12	9-14

Field Segments

Description	Racking	Orientation	Tilt	Azimuth	Intrarow Spacing	Frame Size	Frames	Modules	Power
35 Modules	Flush Mount	Portrait (Vertical)	22°	180°	0.0 m	1x1	35	35	10.2 kW
25 Modules	Flush Mount	Portrait (Vertical)	22°	180°	0.0 m	1x1	25	25	7.25 kW

Figure 7.12 15kW 35/25 Setup simulation parameters

Wiring Zones

Description	Combiner Poles	String Size
Wiring Zone	12	8-23
Wiring Zone 2	12	9-14

Field Segments

Description	Racking	Orientation	Tilt	Azimuth	Intrarow Spacing	Frame Size	Frames	Modules	Power
40 Modules	Flush Mount	Portrait (Vertical)	22°	180°	0.0 m	1x1	40	40	11.6 kW
20 Modules	Flush Mount	Portrait (Vertical)	22°	180°	0.0 m	1x1	20	20	5.80 kW

Figure 7.11 15kW 40/20 Setup simulation parameters

Wiring Zones

Description	Combiner Poles	String Size
Wiring Zone	12	8-23
Wiring Zone 2	12	15-15

Field Segments

Description	Racking	Orientation	Tilt	Azimuth	Intrarow Spacing	Frame Size	Frames	Modules	Power
30 Modules	Flush Mount	Portrait (Vertical)	22°	180°	0.0 m	1x1	30	30	8.70 kW
30 Modules	Flush Mount	Portrait (Vertical)	22°	180°	0.0 m	1x1	28	28	8.12 kW

Figure 7.14 20kW Setup simulation parameters

7.1.3 Calculations

Power usage information extracted from data sheets for each device.

Refrigerator
Model used: Bomann KG 188.
Yearly usage figure based on 24 hr standard testing.
224 kWh yearly / 365 days = 0.61 kWh daily

Microwave
Model used: Signature UPRM3010ST.
Assumed daily usage is 30 minutes.
1.2 kW * 0.5 hours = 0.6 kWh daily

Television
Model used: LG 49SM8600PUA.
Assumed daily usage is 5 hours, yearly figure taken from energy guide.
124 kWh yearly / 365 days = 0.34 kWh daily

Light 1 (x20)
Model used: Philips LED GLS Lamp.
Assumed usage is 20 lights for 10 hours.
0.01 kW * 10 hours * 20 = 2 kWh daily

Light 2 (x4)
Model used: xavax 5.5W LED Bulb.
Assumed usage is 4 lights used constantly.
0.0055 kW * 24 hours * 4 = 0.53 kWh daily

Electric Kettle
Model used: SPT SK-1717.
Assumed daily usage is 20 minutes.
1.5 kW * 0.2 hours = 0.25 kWh daily

Air Conditioner
Model used: LG S09AWN-14.
Assumed daily usage is 8 hours.
0.52 kW * 8 hours = 4.16 kWh daily

Ceiling Fan (x2)
Model used: Westinghouse 142.
Assumed daily usage is 6 hours.
0.05 kW * 6 hours * 2 = 0.6 kWh daily

Computer
Model used: HP 24 All-in-One PC, this model includes a display and peripherals.
Assumed daily usage is 6 hours at peak power, real world usage will vary as idle power usage is much lower.
0.12 kW * 6 hours = 0.72 kWh daily

Figure 7.15 Calculation of daily loads power usage for design example

7.1.3.1 Calculation of tilt angle:

To calculate the tilt angle of the solar modules, two measurements were taken; one at the highest point of the module and one at the lowest point. The angle was then calculated based on Figure 6.18 using:

$$\sin^{-1}\left(\frac{21}{165.8}\right) = 7.2°$$

The value for the length of the solar module was taken from the datasheet.

Figure 7.16 Height at shortest point

Figure 7.17 Height at tallest point

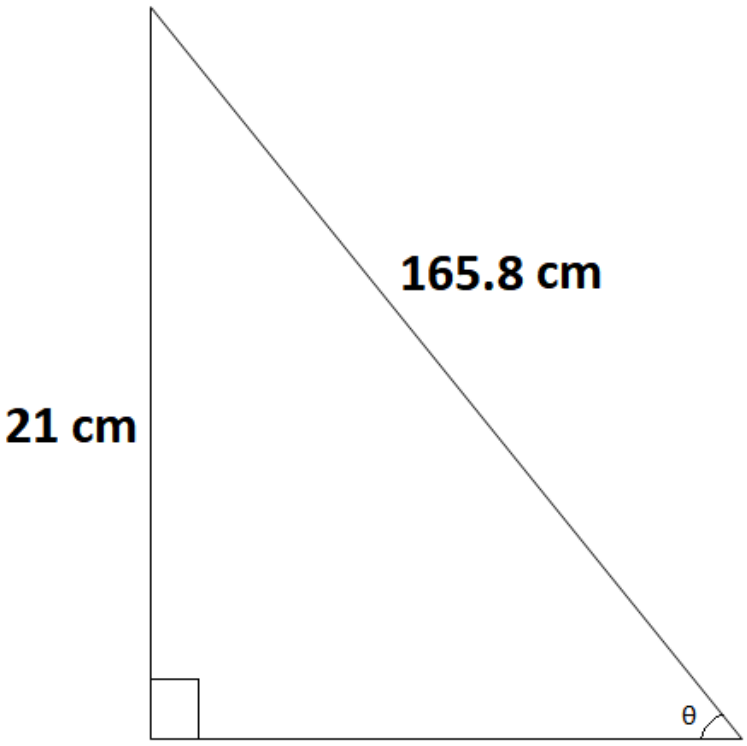

Figure 7.18 Tilt angle calculation

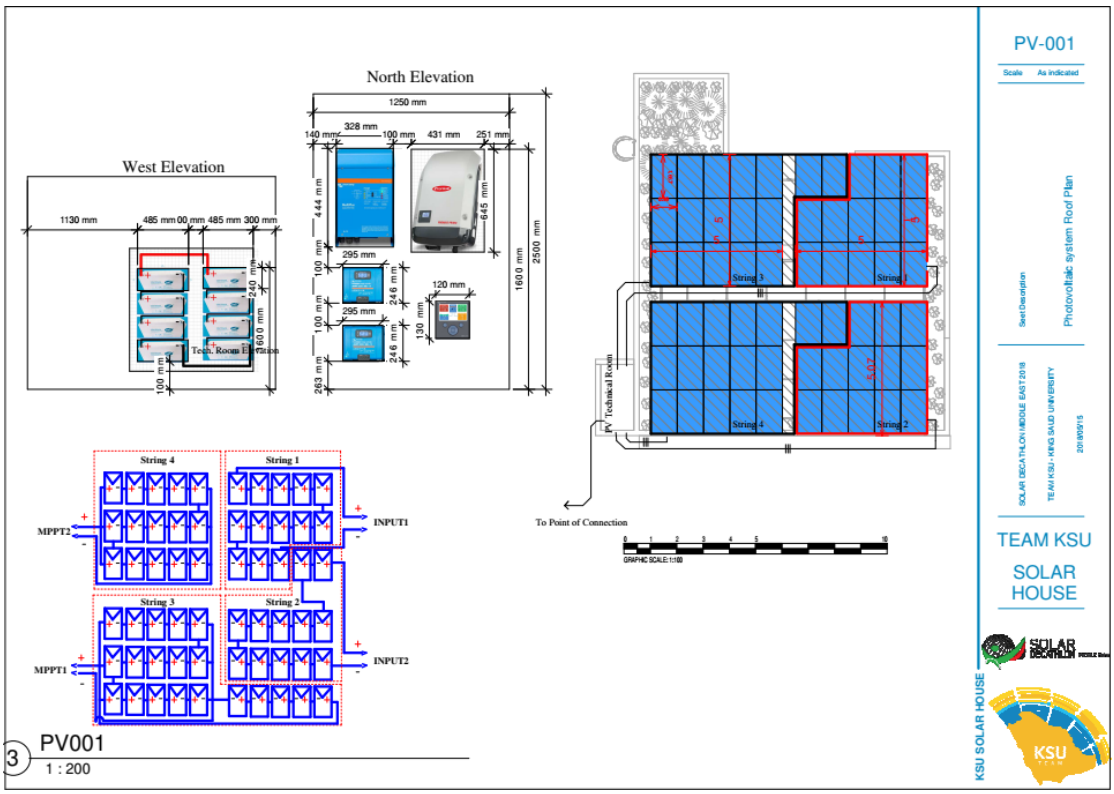

7.1.4 Technical Drawings

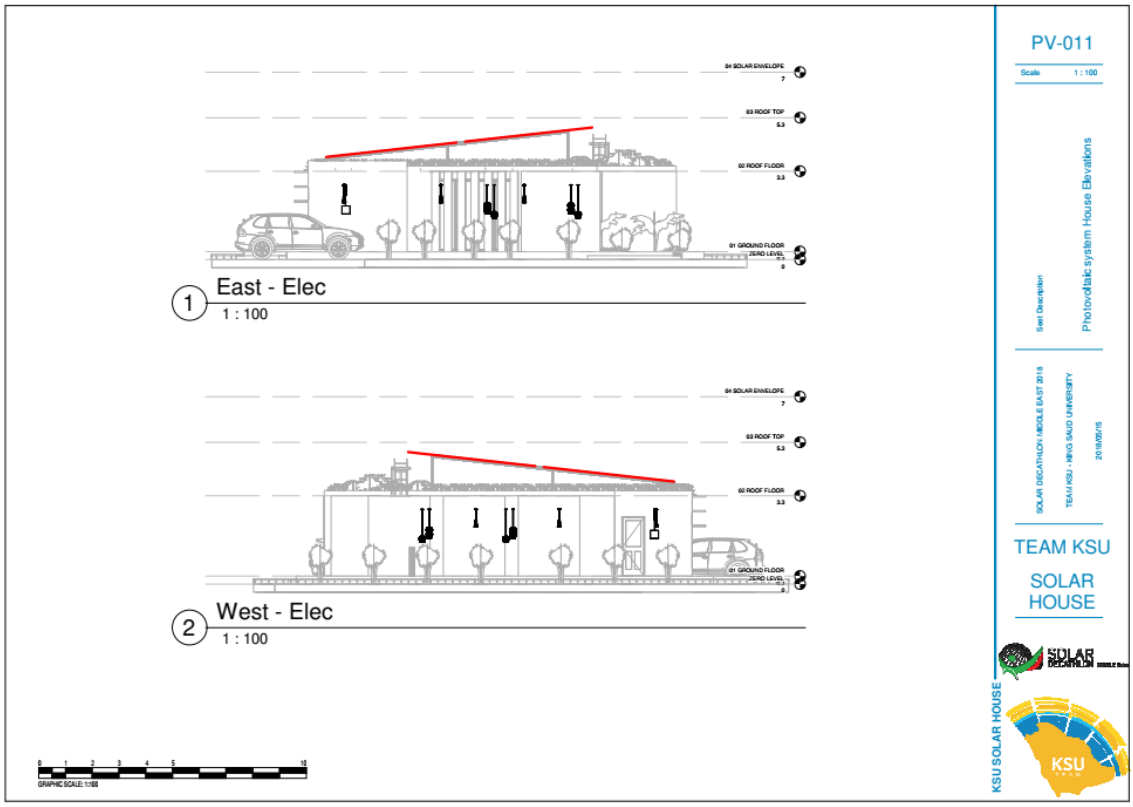

Figure 7.20 PV System String Layout and Technical Room Layout

Figure 7.19 Solar House Elevations

7.1.5 Datasheets

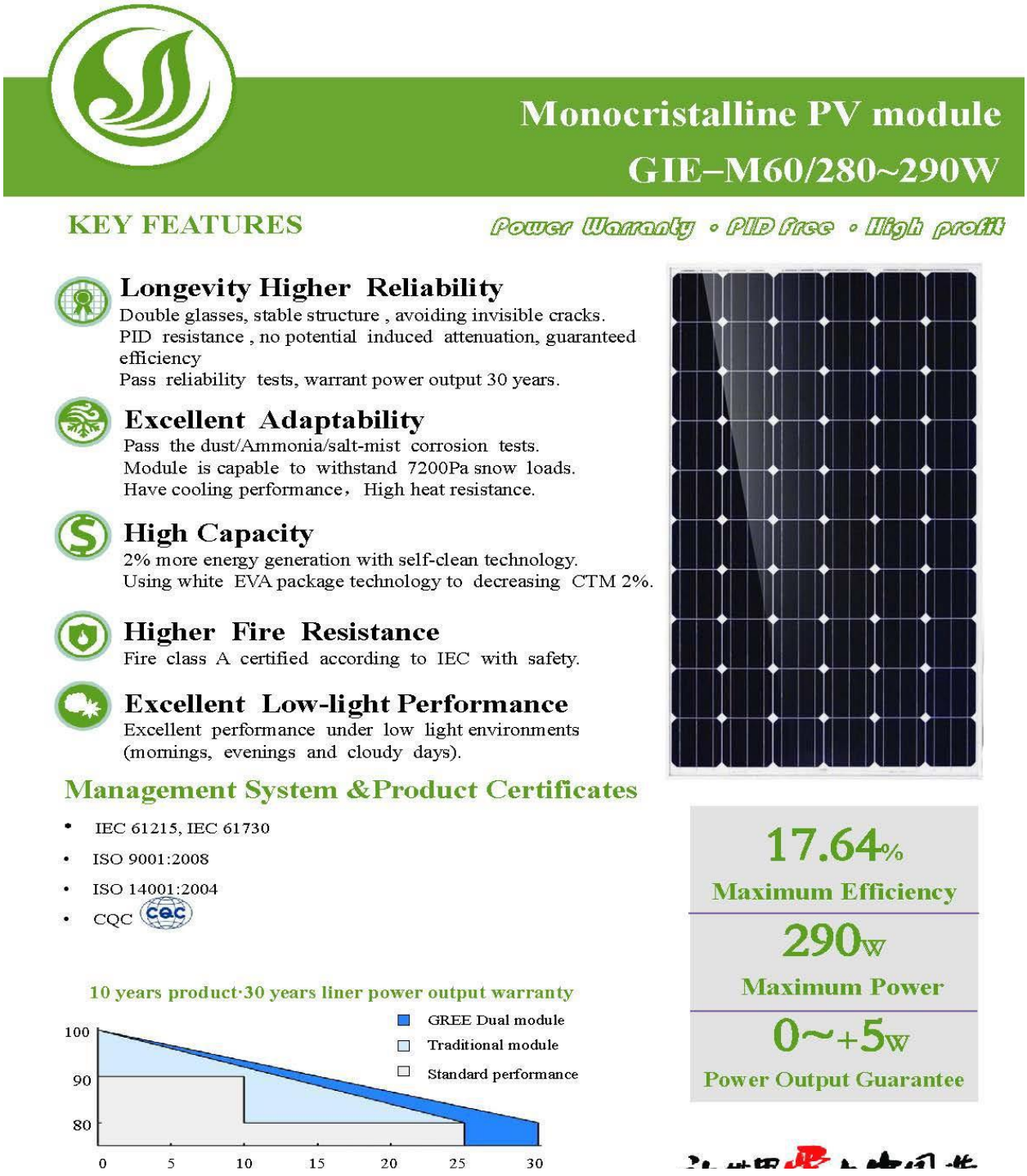

Monocristalline PV module

GIE–M60/280~290W

KEY FEATURES

Power Warranty ◦ PID free ◦ High profit

Longevity Higher Reliability

Double glasses, stable structure , avoiding invisible cracks.
PID resistance , no potential induced attenuation, guaranteed efficiency
Pass reliability tests, warrant power output 30 years.

Excellent Adaptability

Pass the dust/Ammonia/salt-mist corrosion tests.
Module is capable to withstand 7200Pa snow loads.
Have cooling performance， High heat resistance.

High Capacity

2% more energy generation with self-clean technology.
Using white EVA package technology to decreasing CTM 2%.

Higher Fire Resistance

Fire class A certified according to IEC with safety.

Excellent Low-light Performance

Excellent performance under low light environments (mornings, evenings and cloudy days).

Management System &Product Certificates

- IEC 61215, IEC 61730
- ISO 9001:2008
- ISO 14001:2004
- CQC

10 years product·30 years liner power output warranty

17.64%
Maximum Efficiency

290W
Maximum Power

0~+5W
Power Output Guarantee

Figure 7.21 Solar module datasheet page 1

Dual-Glass | Frameless GIE-M60/280~290W

Dimensional Drawings (Units:mm)

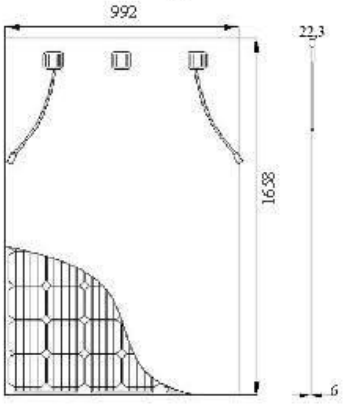

P-V Curve (290W)

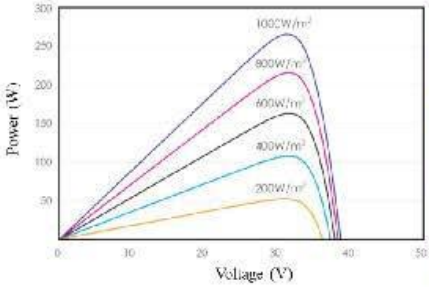

I-V Curve (290W)

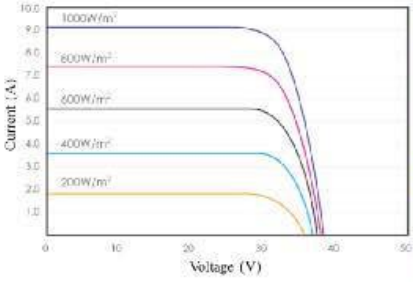

Mechanical Characteristics			
Dimensions (mm)	1658×992×5	1658×992×6	1658×992×7.5
Weight (kg)	19.4	22.5	27
Front/Back Tempered Glass(mm)	2.0	2.5	3.2
Cell Arrangement	60 (6×10)		
J-Box	IP67, Split J-Box		
Connector	MC4 or MC4 Compatible		
Cable Length	Anode 280mm,Cathode 150mm(custom-made)		
Cable	TUV 4mm²		
Packaging Configuration	30 pieces per pallet		

Electrical Characteristics (STC)			
Module Type	GIE-M60/280	GIE-M60/285	GIE-M60/290
Pmax (W)	280	285	290
Vmpp(V)	31.95	32.36	32.76
Impp (A)	8.769	8.805	8.853
Voc (V)	39.22	39.26	39.31
Isc (A)	9.305	9.333	9.384
Module Eff ((%)	17.03	17.33	17.64
STC	Irradiance1000W/m²,Cell Temperature 25℃, AM1.5		

Electrical Characteristics (NOCT)			
Pmax (W)	202.8	206.4	210
Vmpp(V)	28.2	28.4	28.6
Impp (A)	7.19	7.27	7.35
Voc (V)	34.7	34.9	35.1
Isc (A)	7.74	7.83	7.92
NOCT	Irradiance 800W/m², Temperature20℃, AM1.5, Wind speed 1m/s		

Temperature Coefficients (STC)	
Temperature Coefficient (Pmax)	-0.410(%/℃)
Temperature Coefficient (Voc)	-0.330(%/℃)
Temperature Coefficient (Isc)	0.059(%/℃)
Temperature Coefficient (Vmp)	-0.410(%/℃)

Working Conditions	
Operating Temperature	-40~+85℃
RatingSystem Voltage	1500V DC
Series Fuse Rating	14A
ApplicationClass	Class A

Mechanical load resistance selection			
Glass thickness	2.0mm	2.5mm	3.2mm
Front mechanical load	3600Pa(14level)	5400Pa(16level)	7200Pa(17level)
Back mechanical load	2400Pa(12level)	2400Pa(12level)	2400Pa(12level)

Gree Electric Appliances, Inc. of Zhuhai 让天空更蓝 大地更绿

http : //www.gree.com

Add: West Jinji Rd, Qianshan, Zhuhai, Guangdong, China 519070

Figure 7.22 Solar module datasheet page 2

TECHNICAL DATA FRONIUS PRIMO (5.0-1, 5.0-1 AUS, 6.0-1, 8.2-1)

INPUT DATA	PRIMO 5.0-1	PRIMO 5.0-1 AUS	PRIMO 5.0-1 SC	PRIMO 6.0-1	PRIMO 8.2-1
Number of MPP trackers	2				
Max. input current ($I_{dc\ max\ 1}$ / $I_{dc\ max\ 2}$)	12.0 A / 12.0 A	18.0 A / 18.0 A			
Max. array short circuit current (MPP_1/MPP_2)	18.0 A / 18.0 A	27.0 A / 27.0 A			
DC input voltage range ($U_{dc\ min}$ - $U_{dc\ max}$)	80 - 1,000 V				
Feed-in start voltage ($U_{dc\ start}$)	80 V				
Usable MPP voltage range	80 - 800 V				
Number of DC connections	2 + 2				
Max. PV generator output ($P_{dc\ max}$)	7.5 kW_{peak}	7.5 kW_{peak}	7.5 kW_{peak}	9.0 kW_{peak}	12.3 kW_{peak}

OUTPUT DATA	PRIMO 5.0-1	PRIMO 5.0-1 AUS	PRIMO 5.0-1 SC	PRIMO 6.0-1	PRIMO 8.2-1
AC nominal output ($P_{ac,r}$)	5,000 W	4,600 W	5,000 W	6,000 W	8,200 W
Max. output power	5,000 VA	5,000 VA	5,000 VA	6,000 VA	8,200 VA
AC output current ($I_{ac\ nom}$)	21.7 A	21.7 A	21.7 A	26.1 A	35.7 A
Grid connection (voltage range)	1 ~ NPE 220 V / 230 V (180 V - 270 V)				
Frequency (frequency range)	50 Hz / 60 Hz (45 - 65 Hz)				
Total harmonic distortion	< 5 %				
Power factor ($\cos \varphi_{ac,r}$)	0.85 - 1 ind. / cap.				

GENERAL DATA	PRIMO 5.0-1	PRIMO 5.0-1 AUS	PRIMO 5.0-1 SC	PRIMO 6.0-1	PRIMO 8.2-1
Dimensions (height x width x depth)	645 x 431 x 204 mm				
Weight	21.5 kg				
Degree of protection	IP 65				
Protection class	I				
Overvoltage category (DC / AC) [1]	2 / 3				
Night time consumption	< 1 W				
Inverter design	Transformerless				
Cooling	Regulated air cooling				
Installation	Indoor and outdoor installation				
Ambient temperature range	-40 - +55 °C				
Permitted humidity	0 - 100 %				
Max. altitude	4,000 m				
DC connection technology	4x DC+ and 4x DC- screw terminals 2.5 - 16 mm^2				
AC connection technology	3-pole AC screw terminals 2.5 - 16 mm^2				
Certificates and compliance with standards	DIN V VDE 0126-1-1/A1, IEC 62109-1/-2, IEC 62116, IEC 61727, AS 4777-2, AS 4777-3, G83/2, G59/3, CEI 0-21, VDE AR N 4105 [2]				

Figure 7.23 Fronius Primo datasheet

MultiPlus 12 Volt / 24 Volt / 48 Volt	C 12/800/35 C 24/ 800/16	C 12/1200/50 C 24/1200/25	C 12/1600/70 C 24/1600/40	C 12/2000/80 C 24/2000/50	12/3000/120 24/3000/70 48/3000/35	24/5000/120 48/5000/70
PowerControl	Yes	Yes	Yes	Yes	Yes	Yes
PowerAssist	Yes	Yes	Yes	Yes	Yes	Yes
Transfer switch (A)	16	16	16	30	16 or 50	100
INVERTER						
Input voltage range (V DC)	9,5 – 17 V 19 – 33 V 38 – 66 V					
Output	Output voltage: 230 VAC ± 2% Frequency: 50 Hz ± 0,1% (1)					
Cont. output power at 25°C (VA) (3)	800	1200	1600	2000	3000	5000
Cont. output power at 25°C (W)	700	1000	1300	1600	2400	4000
Cont. output power at 40°C (W)	650	900	1200	1400	2200	3700
Cont. output power at 65°C (W)	400	600	800	1000	1700	3000
Peak power (W)	1600	2400	3000	4000	6000	10.000
Maximum efficiency (%)	92 / 94	93 / 94	93 / 94	93 / 94	93 / 94 / 95	94 / 95
Zero load power (W)	8 / 10	8 / 10	8 / 10	9 / 11	20 / 20 / 25	30 / 35
Zero load power in AES mode (W)	5 / 8	5 / 8	5 / 8	7 / 9	15 / 15 / 20	25 / 30
Zero load power in Search mode (W)	2 / 3	2 / 3	2 / 3	3 / 4	8 / 10 / 12	10 / 15
CHARGER						
AC Input	Input voltage range: 187-265 VAC Input frequency: 45 – 65 Hz Power factor: 1					
Charge voltage 'absorption' (V DC)	14,4 / 28,8 / 57,6					
Charge voltage 'float' (V DC)	13,8 / 27,6 / 55,2					
Storage mode (V DC)	13,2 / 26,4 / 52,8					
Charge current house battery (A) (4)	35 / 16	50 / 25	70 / 40	80 / 50	120 / 70 / 35	120 / 70
Charge current starter battery (A)	4 (12 V and 24 V models only)					
Battery temperature sensor	yes					
GENERAL						
Auxiliary output (5)	n. a.	n. a.	n. a.	n. a.	Yes (16A)	Yes (50A)
Programmable relay (6)	Yes					
Protection (2)	a - g					
VE.Bus communication port	For parallel and three phase operation, remote monitoring and system integration					
General purpose com. port	n. a.	n. a.	n. a.	n. a.	Yes	Yes
Remote on-off	Yes					
Common Characteristics	Operating temp. range: -40 to +65°C (fan assisted cooling) Humidity (non-condensing): max 95%					
ENCLOSURE						
Common Characteristics	Material & Colour: aluminium (blue RAL 5012) Protection category: IP 21					
Battery-connection	battery cables of 1.5 meter			M8 bolts	Four M8 bolts (2 plus and 2 minus connections)	
230 V AC-connection	G-ST18i connector			Spring-clamp	Screw terminals 13 mm² (6 AWG)	M6 bolts
Weight (kg)	10	10	10	12	18	30
Dimensions (hxwxd in mm)	375x214x110			520x255x125	362x258x218	444x328x240
STANDARDS						
Safety	EN-IEC 60335-1, EN-IEC 60335-2-29, IEC 62109-1					
Emission, Immunity	EN 55014-1, EN 55014-2, EN-IEC 61000-3-2, EN-IEC 61000-3-3, IEC 61000-6-1, IEC 61000-6-2, IEC 61000-6-3					
Road vehicles	12V and 24V models: ECE R10-4					
Anti-islanding	See our website					

1) Can be adjusted to 60 HZ. 120 V models available on request
2) Protection key:
a) output short circuit
b) overload
c) battery voltage too high
d) battery voltage too low
e) temperature too high
f) 230 VAC on inverter output
g) input voltage ripple too high

3) Non-linear load, crest factor 3:1
4) At 25°C ambient
5) Switches off when no external AC source available
6) Programmable relay that can a.o. be set for general alarm,
DC under voltage or genset start/stop function
AC rating: 230 V/4A
DC rating: 4 A up to 35 VDC, 1 A up to 60 VDC

Figure 7.24 Victron Multiplus datasheet

SmartSolar Charge Controller	250/60	250/70	250/85	250/100
Battery voltage	12 / 24 / 48V Auto Select (software tool needed to select 36V)			
Rated charge current	60A	70A	85A	100A
Nominal PV power, 12V 1a,b)	860W	1000W	1200W	1450W
Nominal PV power, 24V 1a,b)	1720W	2000W	2400W	2900W
Nominal PV power, 36V 1a,b)	2580W	3000W	3600W	4350W
Nominal PV power, 48V 1a,b)	3440W	4000W	4900W	5800W
Max. PV short circuit current 2)	35A (max 30A per MC4 conn.)		70A (max 30A per MC4 conn.)	
Maximum PV open circuit voltage	250V absolute maximum coldest conditions 245V start-up and operating maximum			
Maximum efficiency	99%			
Self-consumption	Less than 35mA @ 12V / 20mA @ 48V			
Charge voltage 'absorption'	Default setting: 14,4 / 28,8 / 43,2 / 57,6V (adjustable with: rotary switch, display, VE.Direct or Bluetooth)			
Charge voltage 'float'	Default setting: 13,8 / 27,6 / 41,4 / 55,2V (adjustable: rotary switch, display, VE.Direct or Bluetooth)			
Charge voltage 'equalization'	Default setting: 16,2V / 32,4V / 48,6V / 64,8V (adjustable)			
Charge algorithm	multi-stage adaptive (eight preprogrammed algorithms) or user defined algorithm			
Temperature compensation	-16 mV / -32 mV / -64 mV / °C			
Protection	PV reverse polarity / Output short circuit / Over temperature			
Operating temperature	-30 to +60°C (full rated output up to 40°C)			
Humidity	95%, non-condensing			
Maximum altitude	5000m (full rated output up to 2000m)			
Environmental condition	Indoor, unconditioned			
Pollution degree	PD3			
Data communication port	VE.Direct or Bluetooth			
Remote on/off	Yes (2 pole connector)			
Programmable relay	DPST AC rating: 240VAC / 4A DC rating: 4A up to 35VDC, 1A up to 60VDC			
Parallel operation	Yes			
ENCLOSURE				
Colour	Blue (RAL 5012)			
PV terminals 3)	35 mm² / AWG2 (Tr models) Two pairs of MC4 connectors (MC4 models)		35 mm² / AWG2 (Tr models) Three pairs of MC4 connectors (MC4 models)	
Battery terminals	35mm² / AWG2			
Protection category	IP43 (electronic components), IP22 (connection area)			
Weight	3 kg		4,5 kg	
Dimensions (h x w x d) in mm	Tr models: 185 x 250 x 95 mm MC4 models: 215 x 250 x 95 mm		Tr models: 216 x 295 x 103 MC4 models: 246 x 295 x 103	
STANDARDS				
Safety	EN/IEC 62109-1, UL 1741, CSA C22.2			

1a) If more PV power is connected, the controller will limit input power.
1b) The PV voltage must exceed Vbat + 5V for the controller to start. Thereafter the minimum PV voltage is Vbat + 1V.
2) A PV array with a higher short circuit current may damage the controller.
3) MC4 models: several splitter pairs may be needed to parallel the strings of solar panels
Maximum current per MC4 connector: 30A (the MC4 connectors are parallel connected to one MPPT tracker)

Figure 7.25 Victron SmartSolar Charge Controller datasheet